



Published in final edited form as:

Adv Biol (Weinh). 2023 April ; 7(4): e2200267. doi:10.1002/adbi.202200267.

Bioengineering and Clinical Translation of Human Lung and its Components

I. Deniz Derman^{1,2}, **Yogendra Pratap Singh**^{1,2}, **Shweta Saini**^{1,3}, **Momoka Nagamine**^{2,4}, **Dishary Banerjee**^{1,2}, **Ibrahim T. Ozbolat**^{*,1,2,5,6,7,8,9}

¹Engineering Science and Mechanics Department, Penn State University; University Park, PA, 16802, USA

²The Huck Institutes of the Life Sciences, Penn State University; University Park, PA, 16802, USA

³Department of Biological Sciences, Indian Institute of Science Education and Research Mohali, India

⁴Department of Chemistry, Penn State University; University Park, PA, 16802, USA

⁵Biomedical Engineering Department, Penn State University; University Park, PA, 16802, USA

⁶Materials Research Institute, Penn State University; University Park, PA, 16802, USA

⁷Cancer Institute, Penn State University; University Park, PA, 16802, USA

⁸Neurosurgery Department, Penn State University; University Park, PA, 16802, USA

⁹Department of Medical Oncology, Cukurova University, Adana, Turkey

Abstract

Clinical lung transplantation has rapidly established itself as the gold standard of treatment for end-stage lung diseases in a restricted group of patients since the first successful lung transplant occurred. Although significant progress has been made in lung transplantation, there are still numerous obstacles in the path of clinical success. The development of bioartificial lung grafts using patient-derived cells might serve as an alternative treatment modality; however, challenges include developing appropriate scaffold materials, advanced culture strategies for lung-specific multiple cell populations, and fully matured constructs to ensure increased transplant lifetime following implantation. This review highlights the development of tissue-engineered tracheal and lung equivalents over the course past two decades, key problems in lung transplantation in a clinical environment, the advancements made in scaffolds, bioprinting technologies, bioreactors, organoids, and organ-on-a-chip technologies. The review aims to fill the lacuna in existing literature towards a holistic bioartificial lung tissue, including trachea, capillaries, airways, bifurcating bronchioles, lung disease models and their clinical translation. Herein, the efforts are on bridging the application of lung tissue engineering methods in a clinical environment as we

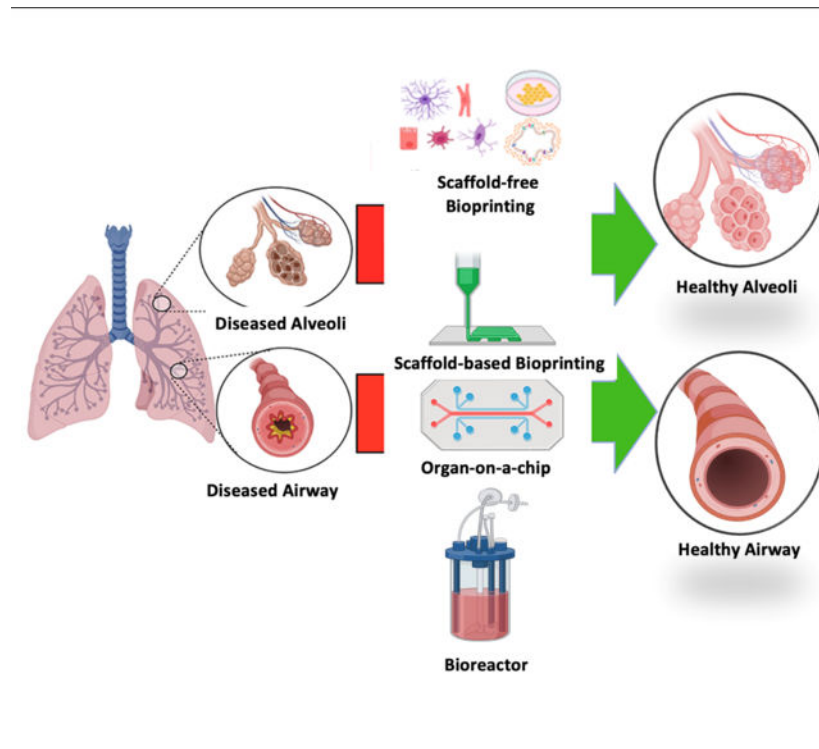
*Corresponding author: Ibrahim T. Ozbolat. ito1@psu.edu.

Contributions. I.T.O., I.D.D, Y.P.S. and D.B. contributed to the conception and design of the paper. All authors contributed on writing and preparation the manuscript and approved the final submitted article.

Competing interests. I.T.O serves as a scientific advisor for Biolife4D and Brinter and owns stock in Biolife4D. Other authors declare that they have no financial interest.

think that tissue engineering holds enormous promise for overcoming the challenges associated with clinical translation of bioengineered human lung and its components.

Graphical Abstract



Chronic respiratory diseases are a leading cause of death globally with limited treatment regimes. Towards this, the review highlights the development of tissue-engineered tracheal and lung equivalents over the course past two decades, key problems in lung transplantation in a clinical environment, the advancements made in scaffolds, bioprinting technologies, bioreactors, organoids, and organ-on-a-chip technologies.

Keywords

Lung; Bioprinting; Transplantation; Trachea; Airways

1. Introduction

Surging pulmonary tract infections threaten to be the biggest healthcare challenges across the globe in the present century. End-stage pulmonary diseases such as chronic obstructive pulmonary disease, cystic fibrosis, pulmonary hypertension, and idiopathic pulmonary fibrosis affect more than 400 million people worldwide, causing about 3 million deaths annually¹. Despite the high prevalence and associated economic burden, the treatment of such acute and chronic diseases is currently limited to symptoms control². Lung transplants have been considered as a treatment regime for combating these end-stage pulmonary diseases, but the orchestra of locating and harvesting a viable lung and chances

of immune rejection and infection control post-transplantation limit the total number of effective annual lung transplantation. Strong immuno-suppressing medications can be used to reduce the immune rejection of donor lungs, but cannot be stopped entirely, along with the unavoidable serious side effects causing kidney damage, vulnerability of infections, and diabetes. After three years of lung transplantation, only 55–70% of the patients are alive³. Thus, even though the first lung transplantation was successful in the early eighties⁴, only 2,000 surgeries have been performed annually in the U.S. compared to ~20,000 kidney transplantations³. The paucity of donor organs, and serious transplant related complications have compelled researchers to use bioengineering approaches to fabricate transplantable lung substitutes. Even though tissue engineering represents an attractive alternative for regeneration of several organ systems, but the complex three-dimensional (3D) architecture of the lung with hollow interconnected airway-alveolar units and pulmonary capillaries makes lung regeneration challenging. Although significant efforts have been made for regeneration of tracheal tissue⁵ and fabrication of micro-physiological models of lung, primarily on Transwell inserts⁶ or in microfluidics devices⁷, no study has demonstrated fabrication of lung tissue spanning from bifurcating bronchioles to alveolar sacs and capillaries, necessary for transplantation purposes.

Anatomically, the trachea starts at the border of the larynx and splits into right and left bronchi at the end, one of which travels to each lung (Fig. 1A). It makes it easier for air to go from the nasopharynx to the bronchi and then to the lungs. Ciliated cells, goblet cells that secrete mucus, and mucus-secreting glands make up the tracheal epithelium. Since a significant number of the epithelial cells in the tracheobronchial area are ciliated, the central airways are almost entirely covered with cilia. The bronchi are further divided into bronchioles, which branch in the lungs to create air channels, inside each lobe of the lungs⁸. With terminal bronchioles, the tiniest airways devoid of alveoli, the conducting zone comes to an end⁹. These bronchioles' primary job is to allow air to enter and exit the lungs during breathing^{10,11}. The alveolar sacs, which are sealed off at their edge by a collection of alveoli, serve as a representation of the area where gas exchanges take place¹¹. The principal tasks of the lung are to circulate air, provide oxygen to the blood, and remove carbon dioxide from the circulation. The lung is specially made to carry out these tasks. For this reason, the pulmonary anatomic compartments are tightly linked, and the redundancy of the structures as well as the facilities for collateral ventilation and blood flow allow the lung to quickly adapt to physiologic demands and meet the challenges given by disease¹². The intricate three-dimensional anatomical structures have made them difficult to replicate these tissues.

Even though several reviews have individually focused on the clinical transplantation perspective or the tissue engineering aspect for lung regeneration^{13–16}, to the best of our knowledge, no comprehensive review is based on bridging the gap using lung tissue engineering approaches (Fig. 1B) in a clinical setting. Here, this review aims to discuss tracheal and lung tissue engineering paradigm, shed light on the progress made in scaffolds, organ-on-a-chip devices, stem cells, and highlight the major challenges towards the transplantation of tissue engineered trachea and lung in a clinical setting.

2. Progress in Tracheal Tissue Engineering

Breathing is a natural process that is trachea related and people perform all the time without thinking. However, for people who suffer from trachea-related diseases or damages, the obstruction of breathing leads to poor quality of life and is sometimes fatal. The trachea, or windpipe, is a membranous tube, present between the larynx and lungs, and acts as a conduit to enable breathing. The cells that make up tracheal tissue include epithelial, chondrocytes, endothelial, and smooth muscle cells¹⁷. Tracheal injury can develop due to various reasons - including trauma, inflammation, tumor, and inborn disorders, all of which induce tracheal constriction or cartilaginous tissue damage. In such cases, tracheal allografts have been the only treatment regime of choice. However, surgical intervention with allogenic tracheal conduits is only possible for an allograft of considerable length. A longer length of the intervention, particularly when over 6 cm of the trachea, needs to be excised and replaced, which becomes impossible due to the high mechanical tension generated at the anastomosis site during surgical procedures and thus have the possibility of undesirable results¹⁸. Alongside, high medical cost, lifelong dependency on immunosuppressant drugs, higher susceptibility to infection, and poor quality of life calls for tissue engineering approaches to develop tracheal conduits (a layer of motile ciliated epithelium supported by a layer of cartilaginous vascular tube)¹⁹, with the ability to repair and vascularize without causing an orchestra of immune rejection reactions^{20,21}.

The first effort of a heterotopic/orthotopic tracheal transplantation in humans was reported in 1979, where the trachea graft was integrated into the physiological system and functioned without any complications or immune rejection for nine weeks²². However, the first effort on engineered trachea regeneration did not take place until 1994²³. While the first tissue-engineered trachea temporarily functioned in a patient, it was hampered by a long repair period, revascularization, and dependency on donor tissue²⁴. In this regard, decellularized tissue from patients have found some respite with chances of lesser immune rejection. However, the decellularized scaffolds' reliance on donor tissue is a significant constrain and a synthetic build may be a preferable long-term objective for this purpose.

2.1 3D Printing of the Trachea

In the context of biofabrication, "3D printing" refers to the layer-by-layer fabrication of tissue constructs or scaffolds according to a computer-aided design (CAD) model without using any cells during the process, which can be seeded later. It is promising in terms of customized airway reconstruction and provides an opportunity to construct trachea substitutes with the help of biological and synthetic materials that matches the morphology of the patient's trachea²¹. Biocompatible 3D structures similar to the native trachea with ciliated respiratory mucosa and sufficient cartilage remodeling are necessary for successful tracheal repair. A variety of approaches, mostly using different scaffolds, have been explored for tracheal reconstruction. Park et al. developed a 3D printed monolithic hollow bellows scaffold as a framework for a tissue-engineered trachea²⁵. The engineered trachea was created by seeding chondrocytes on functionalized gelatin sponges into the grooves of bellows scaffold, which showed mechanical properties similar to that of the native trachea along with significant regeneration of tracheal cartilage in vivo. Additionally, they observed

that the use of human turbinate mesenchymal stromal cell (hTMSC) sheets with 3D printed polycaprolactone (PCL) scaffolds improved tracheal epithelialization in non-circumferential tracheal lesions of approximately 5-mm wide and 15-mm long on the anterior tracheal wall in a rabbit model²⁶. However, the study did not consider the segmental tracheal defect for reconstruction assessment.

It has been demonstrated that the presence of mesenchymal stem cells (MSCs) on tracheal scaffolds enhances the development of new tissue following implantation. In this regard, Chang et al. first tested the feasibility of using fibrin/MSC-coated 3D printed PCL scaffolds in the reconstruction of a partial tracheal lesion of approximately 10 mm wide by 10 mm long in a rabbit model²⁷. Bone marrow-derived MSCs (BM-MSCs) were extracted from rabbits and seeded in fibrin, which was later used to construct the graft with PCL as a scaffold material. The graft was then implanted in rabbit tracheal defects. Bronchoscopic examination after eight weeks of implantation revealed the defect reconstruction. Histological examination showed that the graft could maintain its shape and successfully integrate with the native trachea. Neo-cartilage was also formed during the successful reconstruction of the trachea without any collapse or occlusion. Regeneration of cilia with a beating frequency like that of the native mucosa was also observed. The study opened the possibility of using other cell types such as chondrocytes for tracheal regeneration. Several researchers explored collagen and gelatin-based scaffolds owing to their mechanical stability. For example, Goldstein et al. used PLA, mature chondrocytes, and collagen type-I to design a 3D printed patch of 8-mm in length, 3-mm in width and 1.2-mm in depth for laryngotracheal reconstruction (LTR)²⁸. Chondrocytes from the tracheal rings of a donor rabbit were isolated and injected into 3D printed PLA scaffolds. The graft was implanted into a rabbit by creating a 3-cm vertical midline incision through skin. The rabbit implanted grafts revealed cartilage tissue formation without significant inflammation or granulation with the presence of mucous in tracheal lumen and newly formed cartilage at the place of the graft. However, no control group was used in this study, which is required along with a longer follow-up study to translate this approach for clinical use. Gao et al. 3D printed biodegradable reticular PCL scaffolds like the rabbit's native trachea²⁹. The 3D printed scaffolds were cultured with chondrocytes for 2 and 4 weeks and were called Group I and II, respectively. The chondrocyte seeded scaffolds were implanted subcutaneously into nude mice, which showed the development of mature tracheal tissue. Further, towards repairing segmental tracheal defects, a large portion of the rabbit's trachea corresponding to the size of the engineered trachea, i.e., 1.65-cm long and 5-mm luminal diameter with 6 convolutions, each of 1.5 mm thickness and 1.5 mm distance between each convolution, was replaced by tissue-engineered trachea, which showed a mean survival time of 14 ± 5 days in Group I and 23 ± 16 days in Group II. Autopsy revealed factors such as pneumonia and infection in the scaffold responsible for the death of rabbits. However, no structural collapse was observed, which means that the tissue-engineered trachea supported the structural integrity.

PCL offers appealing mechanical strength for tracheal defect grafts and can be stable for up to 24 months. In this regard, Townsend et al. fabricated electrospun patches of PCL and polylactide-co-epsilon-caprolactone (PLCL) enclosing 3D printed PCL rings, which were implanted into diamond-shaped rabbit tracheal defects of an approximate size of 15×5

mm for a 12-week implantation study³⁰. The cell adhesion peptide, RGD (Arg-Gly-Asp), or antimicrobial compound, ceragenin-131, were added to the electrospinning solutions, to improve cell adhesion and antimicrobial activity, respectively. The four groups used in the animal study were: 1) PCL-only group (baseline comparator group), 2) faster degrading material PCL/PLCL group, 3) PCL/PLCL with the embedded antimicrobial compound ceragenin-131 (PCL/PLCL+CSA) group, and 4) PCL/PLCL with the cell adhesion peptide RGD (PCL/PLCL + RGD) group. The results showed that the luminal side of the defect had been re-epithelialized. The lumen volume of the PCL/PLCL patches did not significantly differ from that of the uninjured positive control. The last group had significantly greater minimum cross-sectional area as compared to the PCL-only group but comparable to the uninjured positive control. The use of antimicrobial compound, ceragenin-131 (CSA), decreased bacterial growth in vitro, but it had no discernible benefit in vivo. Overall, there was minimal tissue overgrowth and enough tissue in-growth inside the patch material suggesting its feasibility in tracheal repair.

2.2 3D Bioprinting of the Trachea

Bioprinting can be defined as the prescribed layer-by-layer deposition of living cells and other biologics (proteins, growth factors, genes, etc.) laden in biomaterials (bioinks) for various applications such as tissue engineering, drug screening and disease modelling. In the context of biofabrication, the main difference between 3D printing and bioprinting is that 3D printing is performed in an acellular manner while cells and/or other biologics are utilized in bioprinting. The bioinks for 3D bioprinting may be made from several natural or synthetic biomaterials alone, or a combination^{31,32}. To bioprint tissue constructs, both scaffold-based and scaffold-free techniques have been used³³. The scaffold-based approach relies on the use of a suitable biocompatible biomaterial (natural or synthetic) based scaffolds to fabricate tissues, while the scaffold-free approach is based on the assembly of building blocks such as cellular aggregates (i.e., spheroids, cell sheets, etc.) to fabricate tissues³⁴. Here, we outline several of these techniques towards bioprinting of the trachea.

2.2.1 Scaffold-based Techniques—3D Bioprinting has an extra advantage of using cell-laden hydrogels that allows for cell growth and expansion along with the mechanical strength provided by the scaffold. The selection of the right scaffold materials is crucial for cells to behave in the desired manner, including attachment, differentiation, proliferation, cell infiltration, and vascularization. Along with these, the reconstructed trachea should have adequate mechanical strength to match with that of the native trachea³⁵. Biomechanical characteristics should match the compression and stiffness characteristics of the cartilage, connective tissue, and smooth muscle. Bioprinted constructs should be rigid enough to prevent the collapse of the trachea (along with the elasticity for proper movement)³⁶ and biocompatible (non-toxic for cells and not leading to an immune reaction after implantation)³⁷, and possess an appropriated biodegradation rate and the byproducts of degradation should also be non-toxic. The selected biomaterials should provide a frame that could support and maintain ECM with the ability to degrade at an even and slow rate, thus allowing the neighboring cells to recover its supporting functions³⁷. Collagen³⁸, Pluronic F-127³⁹, polyglycolic acid⁴⁰, and PCL⁴¹ have all been employed in fabrication of scaffolds, either alone or in conjunction with other biomaterials^{41,42}. For example, Ke et

al. reconstructed the trachea using two distinct scaffold designs for cartilage and smooth muscle cells using PCL dispensed at a pressure of 700 kPa from a metal nozzle and human MSCs-laden hyaluronic acid (HA) hydrogel dispensed at a pressure of 100 kPa from a Teflon nozzle, via extrusion-based bioprinting⁴³. Transforming growth factor beta 1 (TGF- β 1) was used for inducing smooth muscle formation and chondrogenic differentiation medium for chondrogenesis purposes. The final composition of the hydrogel included 0.1% w/v 2-hydroxy-4'-(2-hydroxyethoxy)-2-methylpropiophenone, dissolved in control medium, chondrogenic medium, and TGF- β 1 supplemented medium as the stock solution of control, cartilage, and smooth muscle hydrogels, respectively. For crosslinking, the acrylate or alkyne solutions were prepared by mixing different concentrations of crosslinkers in hydrogel stock solutions. Hyaluronic acid (HA)/gelatin mix had a final concentration of 1.5 mg mL⁻¹ and 30 mg mL⁻¹, respectively. A substrate elasticity of 5–10 kPa derived the differentiation of human MSCs towards smooth muscle formation and 1–5 kPa for chondrogenesis. The in vitro study at week 4 showed cartilage and smooth muscle formation in bioprinted constructs. The bioprinted tracheal ring had an inner diameter of 20 mm, an outer diameter of 26 mm, and a height of 5 mm, which were obtained from CT images.

In another approach presented by Almendros et al., a suitable bioink was formulated using lung-derived MSCs obtained from Sprague-Dawley and decellularized porcine lung ECM to study cell-matrix cross talk when bioprinted with Pluronic F-127 as a structural and sacrificial hydrogel⁴⁷. More than 90% viability of MSCs was observed and a homogenous distribution of cells was noticed on the matrix. Cells cultured on the lung ECM showed greater adhesion and longer focal adhesions. Additionally, the expression of the C-X-C chemokine receptor type 4 (CXCR4) was more than 20-fold higher in 3D as compared to 2D. Bae et al. conducted an in vivo study of a bioprinted trachea in New Zealand rabbits with a half-pipe-shaped partial tracheal resection of approximately 10 × 10 mm size (Fig. 2A)⁴⁴. They used PCL and differentiated rabbit MSCs loaded in alginate for bioprinting as alternate layers to construct tracheal grafts. PCL was dispensed through a 300 μ m nozzle at a temperature of ~100 °C and a pneumatic pressure of 400 kPa. Two different types of cells were used in the alginate layer, separated by a nonporous PCL layer in the middle that provided the mechanical strength. The outermost and innermost porous PCL layers were responsible for nutrient transport. The artificial trachea had five layers with an inner and outer diameter of 5 and 10 mm, respectively, and a length of 15 mm. Alginate hydrogel was crosslinked using 1% calcium chloride solution and contained 1 × 10⁷ cells/10 mL, which was then dispensed through a 400 μ m nozzle with a pneumatic pressure of 100 kPa at room temperature, with a printing speed of 200 mm/min for all layers. The grafts were then implanted for 12 weeks. During the time course, no respiratory complication or stenosis was observed. Histopathological analysis revealed that the PCL layer was responsible for providing the mechanical support and nutrient transport while the alginate layer contained rabbit respiratory epithelial cells and chondrocytes. Localized neo-cartilage formation and epithelial mucosa were also detected. Expressions of chondrogenic-differentiation markers, such as SOX-9, aggrecan, Col1 α 1 and Col2 α 1, were upregulated in the differentiated BM-MSCs. Long-term in vivo observation of the same study was conducted by Park et al. using PCL and alginate hydrogel with nasal epithelial and auricular cartilage cells⁴⁵. The bioprinted tracheal grafts were implanted in New Zealand rabbits with a cut onto the ventral

portion of trachea into a semi-cylindrical shape measuring approximately 1.5×1.5 cm (Fig. 2B), where neonatal cartilage formation was observed after 6 and 12 months. Radiographs taken right away following the surgery revealed an increase in opacity at implant locations in all rabbits. The average diameter ratio in the control group was $46.19 \pm 22.10\%$, which was higher than the $11.72 \pm 13.81\%$ seen in the experimental group. In particular, the 12-month observation group's rate of tracheal diameter decline was $6.72 \pm 1.07\%$, which was roughly equivalent to the diameter of a healthy trachea. Immature cartilage islets were observed at 6 months, but no cartilage ring formation was identified. Thus, further studies are required for demonstration of cartilage regeneration.

Despite their several benefits, the use of scaffolds has associated challenges as well, such as the risk of infections, reduced biocompatibility, and material degradation over time⁴⁸. These drawbacks limit the clinical translation of 3D printed scaffolds⁴⁹. Materials used in scaffolds have degradation rates that cannot be appropriately synchronized with the formation of new tissue, which leads to a loss in mechanical integrity⁵⁰. Cell viability also decreases due to harsh techniques such as spinner shear, high temperature, and exposure to polymerizing chemicals during the formation of scaffolds. Due to the presence of materials, there is a decrease in cell-to-cell interactions and an alteration in the phenotype of cells, resulting in a decrease in the rate of ECM production^{51,52}. The presence of materials also decreases cellular density and obstructs mechanotransduction⁵³. Even after the transplantation, scaffolds can release toxic byproducts that can lead to immunogenicity and inflammation⁵⁴.

2.2.2 Scaffold-free Techniques—The scaffold-free approach is advantageous in terms of eliciting less inflammation as observed in the scaffold-based approach because foreign biomaterials are not involved in the biofabrication process. However, this method may jeopardize mechanical integrity. Many scaffold-free techniques rely on a temporary stent to keep the trachea in shape.

The first feasibility study of the scaffold-free approach for tracheal bioprinting was published by Taniguchi et al., where chondrocytes (isolated from rib cartilage of Fisher rats), BM-MSCs, and commercial rat lung micro-vessel endothelial cells were utilized to create heterocellular spheroids⁵. Next, the Regenova Bio3D printer was used to form tracheal constructs, which were further kept in a bioreactor for maturation and then implanted in F344 rats, having a defect size of 4.82 ± 0.81 mm with a silicone stent to support the trachea. Along with the mechanical integrity, the grafts also showed the formation of connective tissue and capillaries. Epithelization started at Day 8 but was not completed until Day 23. The grafts also led to thick secretions, coughing, granulation due to the presence of stents. The study paved the way for the scaffold-free approach, but a long-term follow-up study in large animals is needed for clinical viability. Machino et al. continued this strategy using human cells that led to native-like trachea of thickness and length of ~ 550 μm and 5 mm, respectively (Fig. 2C)⁴⁶. Human chondrocytes, hMSCs, human fibroblasts and human umbilical vein endothelial cells (HUVECs) were cocultured to form spheroids, having property of both rigidity and flexibility, which were bioprinted to create a ladder-like individual cartilaginous and fibrous tubes. Results exhibited the presence of epithelial cells and blood vessels, after seven days of implantation into rats, although granulation was

also observed initially but disappeared later indicating healing. However, the structure was not strong enough to maintain its shape after continuous breathing, thus the stent during transplantation was required. The stent was not removed during the study thus a long-term follow-up study after removing the stent is required.

Reproducible fabrication of cell aggregates in a robust and high-throughput manner holds the key to create these scaffold-free constructs at the human scale, according to another study⁵⁵. Vascularization of these constructs have been found to play a key role for improved in vivo performance. Isolation of endothelial cells from adult tissues is difficult and hampers the biological functioning of epithelial cells. Alternatives include endothelial cells derived from stem cells, such as induced-pluripotent stem cells (iPSCs). For example, Taniguchi et al. demonstrated that iPSC-derived endothelial cells had similar tensile strengths in the airway constructs compared HUVECs, showing the potential of iPSC-derived endothelial cells in replacing HUVECs in tracheal reconstruction⁵⁶. Nevertheless, the group concluded that iPSC-derived endothelial cells have certain limitations including being vulnerable to apoptosis in scaffold-free architectures.

2.3 Bioreactors for Trachea

The conventional static culture techniques have some drawbacks, such as the inability to provide cells with a homeostatic environment with periodic manual changing of medium leading to abrupt changes in culture conditions, such as pH and nutrients, reducing the viability of cells. Especially for clinical purposes, manual culture techniques for generation of physiologically-relevant cell densities lead to longer development time, increased cost, and technical or other human errors. Alongside, manual seeding of cells on a scaffold is non-efficient, prone to error, and can lead to non-homogenous cell distribution on scaffolds⁵⁷. To compensate for these drawbacks, bioreactors have been proven to be a suitable option⁵⁸. Bioreactors can provide cells with the required native-like microenvironment and is an easy-to-handle, standardized, and cost-effective way to generate scalable tissues for easy translation from bench to bedside. While bioreactors provide a dynamic way of adding cells required for thicker scaffolds and low porosity, they also enable automatic replenishment of the exhausted media and prevents workforce eliminating human-generated errors. In bioreactors, cell seeding parameters, such as cell concentration in seeding suspension, medium flow rate, flow directions, and timing of perfusion pattern rely on computational methods making it more precise than manual settings. Thus, bioreactors are being used for clinical practices of tissue grafts, as it is cost effective, suitable for patients, and environment friendly way of scaling up cells⁵⁹.

Lin et al. showed that chondrocytes seeded on PCL/collagen composite scaffolds and grown in a rotational bioreactor had a higher proliferation rate, increased matrix secretion, and aligned along the flow direction, confirming that shear stress plays an important role in regulating cell function⁶⁰. The tested constructs, however, was only seeded with chondrocytes and did not have an epithelial lining. The first reported tissue-engineered trachea transplanted in a clinical setting was also cultured in a specially designed bioreactor. Macchiarini et al. designed a bioreactor with two compartments enabling simultaneous culture of different types of cells²⁴. They used a decellularized tracheal

segment obtained from a 51-year-old donor, recipient's bronchiole epithelial cells as the internal surface and recipient's MSC-derived chondrocytes as the external surface. The bioreactor used a polysulphone chamber to house the medium and rotated the airway construct around its longitudinal axis in culture medium. It moved cells alternately between liquid (medium) and gaseous (air) phases (1–1.5 revolutions per min). The bioreactor culture was performed for 96 h, after which it was implanted in a 30-year-old woman, suffering from hypoxia. The implanted graft was phenotypically like the native trachea, with evidence of revascularization. No inflammation or anti-donor human leukocyte antigen (HLA) antibodies or complications were noted in the patient during the period of observation (3 months). This study provided a way that can help in addressing the tracheal implantation combining autologous cells and a bioreactor at the clinical level.

Zhou et al. reported implantation of a bioengineered lung graft into porcine trachea using decellularized porcine lung scaffold seeded with human epithelial and endothelial cells⁶¹. The graft could withstand the recipient's blood flow and showed gaseous exchange when observed for 1 h after implantation, with no observation provided after that point. Ghaedi et al. used a rotating bioreactor to mimic the physiological environment by enabling the air-liquid interface (ALI) that helped differentiate iPSCs into alveolar epithelial cells. The study helped in using autologous cells for constructing a bioengineered trachea⁶².

Engineered trachea will always need a dynamic bioreactor system enabling fluid and gas perfusion to mature tissues before transplantation. Such a reactor has the capacity of providing independent access lines for providing physiological stimuli for vascularization and airway compartments for oxygen or nutrient delivery. Providing such a microenvironment in an automated manner is deemed economic, with repeatability and lower risks of contamination.

Tissue engineering has advanced significantly since the first bioreactor was designed. The primary tasks that a bioreactor must do include supplying metabolites, such as oxygen and nutrients, eliminating catabolites, regulating temperature, establishing, and monitoring pH, providing mechanical stresses that drive the creation of the ECM, and enabling cohesion between cells. Bioreactors can result in the development of well differentiated 3D tissues with distinct mechanical characteristics by creating and sustaining pseudo-physiological conditions that are particular to and necessary for cell activities.

2.4 Trachea-on-a-chip

In addition to the efforts made for engineering trachea for regenerative medicine purposes, organ-on-a-chip platforms have raised considerable interest for developing micro-physiological systems for airways. For example, Si et al. designed an airway-on-a-chip for testing drug delivery. They tried to mimic the human airway by introducing airway specific cells into it. They designed a microfluidic device, having two parallel microchannels separated by an extracellular matrix coated porous flexible membrane made of polydimethylsiloxane (PDMS), with a pore size of 7 mm. Primary human lung bronchial-airway basal stem cells were cultured under air-liquid interface (ALI) on one membrane side. In contrast, primary human lung endothelial cells were cultured on the opposite side of the same membrane and exposed to a continuous flow of culture media.

The device supported the differentiation of lung bronchial-airway basal stem cells into mucociliated, pseudostratified bronchial-airway epithelium. Other airway-specific cell types such as ciliated cells, mucus-producing goblet cells, club cells, and basal cells were also identified in some proportions⁶³. Along with it, ZO-1 tight junction, cilia, and mucous were also present. The differentiated airway epithelium in the chip expressed higher levels of genes encoding multiple serine proteases, including TMPRSS2, TMPRSS4, TMPRSS11D, and TMPRSS11E (DESC1), that are involved in the entry of influenza virus in vivo. The microfluidic device could mimic the influenza disease model, which was confirmed by the disruptions of tight junctions, loss of apical cilia, and compromised barrier function when infected with green fluorescent protein (GFP)-expressing influenza A/PuertoRico8/34 (H1N1) virus. Loss of VE-cadherin-containing adherent junctions confirmed the disruption of the lung endothelium on the chip, which is also observed in vivo by vascular leakage. The recruitment of these cells also confirmed pathology during the infection of the chip's apical surface of the activated lung endothelium within minutes. Clearance of the virus was evident by a decrease in the GFP⁺ cells in 1–2 days. Due to its ability to mimic diseases that found in vivo, the chip platform can be used for drug testing as well. However, looking at a few reported literatures in this area, there is clearly much progress to be made towards developing trachea-on-a-chip models.

2.5 Vascularization in Tracheal Grafts

Vascularization is critical for the survival of tracheal grafts, especially when grafts are large and thick, because diffusion is insufficient to meet metabolic demands⁶⁴. It maintains an adequate blood supply to avoid necrosis of tracheal grafts, which can result in a variety of complications, including the formation of granulation tissue and stenosis, both of which are fatal. While the fabrication of tissue-engineered tracheas has been investigated, they are often not vascularized before their implantation. There is no easy or obvious solution to revascularization, and scientists have debated on whether pre-vascularization is required⁶⁵. To preserve construct viability, tracheal grafts require at least some degree of vascularization and future tissue-engineered tracheas must entail a vascularization strategy.

Decellularization and recellularization have been often used in combination to circumvent vascularization problems. In decellularized grafts, Walles et al. addressed vascularity problems by conserving the vascular pedicle and perfusing the pedicle with endothelial cells^{66,67}. Another method of revascularization is to encapsulate an engineered graft with vascularized tissue. Epithelial cells separated from abdominal skin patch from 10 mongrel dogs after culturing in vitro for 4 weeks were seeded onto a porous polylactic glycolic acid (PLGA) scaffold (6 × 8 cm) for constructing lining mucosa, which was further mounted on a prosthesis framework made of polypropylene mesh, the PLGA-gelatin and polypropylene prosthesis was then integrated to omentum and implanted into a circumferential defect in the same dog's trachea⁶⁸. Due to a sophisticated isolation process, obtaining an omentum scaffold itself is too difficult; nevertheless, once transplanted into the trachea, the omentum derived constructs retained their vascularized structure even after a month. Luo et al. implanted tracheal scaffolds intramuscularly in the sternohyoid muscle for four weeks in a rabbit model to prevascularize the graft⁶⁹. In comparison to static culture, Haykal et al. used a bioreactor to seed epithelial cells and BM-MSCs to the luminal and external surfaces of

a decellularized tracheal graft, respectively, and discovered that cell attachment was higher and cell distribution was even more when compared to the heterogenous cell distribution during traditional seeding methods such as static seeding⁷⁰. On postoperative Day 3, they were unable to detect labeled cells on the luminal surface and surrounding cartilage, and no epithelium formation was observed in the first two weeks following transplantation. This demonstrated that despite the increased cell number, the tracheal graft was unable to support cell survival in vivo, owing to a lack of vascular support. The implantation of a tracheal shaped high-density polyethylene structure painted with chondrocyte-laden Pluronic F127 hydrogel, with a cell density of 3×10^7 cells per ml hydrogel, on the outer surface in an athymic mouse resulted in the formation of a tissue construct resembling mature hyaline cartilage after eight weeks using the body as a bioreactor⁷¹. Kajbafzadeh et al. used a decellularized tracheal graft to recellularize the construct in a mouse⁷². The graft was harvested 12 months after it was implanted and revealed well-organized cartilage and connective tissue formation as well as blood vessels. Nonetheless, the epithelial layer was not regenerated in either study, or the graft's suitability for tracheal replacement was not tested.

Thus, the tracheal vasculature not only ensures a physical barrier between the blood and tissue but also metabolically controls the exchange of nutrients, oxygen diffusion and control of macromolecules diffusion⁷³. Still, tissue-engineered tracheal constructs face several roadblocks with the need for an appropriate endothelial cell population, and culture and seeding strategies. Alongside, the significant phenotypic heterogeneity in the tracheal vasculature necessitates the isolation of endothelial cells from the trachea itself. However, the allogeneity of endothelium initiates an orchestra of immune reactions. iPSC-derived endothelial cells offer an alternative solution, but more specific research is needed towards understanding the phenotypic differences between lung-specific endothelial cells and iPSC-derived endothelial cells.

2.6 Critical Concerns

Belsey, Neville et al., and Grillo have summarized the requirements for an ideal tissue-engineered trachea^{19,20,18}. The most important requirements are a lateral rigid property to provide adequate strength to the trachea to prevent its collapse, combined with longitudinal flexibility to ensure normal head and neck activity. The tracheal grafts developed till now have not been able to mimic the rigidity and flexibility of the native trachea. Researchers investigate different biocompatible materials that can help provide flexibility to tracheal grafts and possibly mimic the native trachea⁷⁴. A sufficient respiratory epithelium is also required to provide a barrier against infections and to move foreign particles out of the trachea. To overcome the shortage of donor organs, the materials and cells required for tissue-engineered trachea should be easily accessible and available. The tissue-engineered trachea should be able to grow with the patient in pediatric cases. Complete tracheal re-epithelialization is the most important of these requirements, as it is the primary determinant of the long-term success of a functional tissue-engineered trachea.

Decellularized tracheal grafts are considered a promising candidate for tracheal tissue engineering⁵⁹. The decellularization process must enable the removal of the cellular

components to prevent the host immune response. However, the process of decellularization needs to be optimized. Detergents, such as sodium dodecyl sulfate (SDS) and enzymes (DNAse), are used for the decellularization process, which can alter the physical, biological, and chemical properties and destroy the ECM components, which can further impact the adherence of future cells⁷⁵. Therefore, a suitable duration and method of decellularization are essential. Several difficulties are also faced during the transplantation procedures. Many causes can lead to early death post-transplantation, such as the collapse of the tracheal graft lumen^{76,77}. The collapse can be due to the insufficient mechanical strength and host immune response. Better study on the host immune response before the implantation can help address this problem. Preventing host immune response is making transplantation of tissue-engineered grafts challenging⁷⁸. Thus, to avoid the need for lifelong immunosuppression, an ideal tissue-engineered trachea should have biocompatibility and eventually be accepted by the host⁷⁹.

Proper mechanical strength testing of grafts should be performed under physiological conditions before implantation to avoid collapse. Luminal stents are used to prevent tracheal collapse. The introduction of the stent leads to graft migration that can lead to obstructive stenosis requiring repetitive interventions⁸⁰. Degradable stents can be an alternative, but due to the loss of their functionality, repeated stenting is required⁵⁹. Thus, an ideal graft would have proper mechanical strength without needing any stent. Along with the rigidity, the graft must be flexible enough to accommodate the upper body movements safely. Migration of the graft to neighboring structures can lead to rapid death⁸¹. The migration can also take place to the tracheal lumen leading to airway obstruction, especially the grafts having sharp edges such as metal wires, stents, and meshes that can cause erosion of vessels.

3. Lung Tissue Engineering

While lung is the most susceptible internal organ to airborne infections and injuries due to the constant exposure to the ambient atmosphere, there is a universal shortage of donor lungs resulting in a significant demand for new therapeutic options for lung regeneration. Tissue engineering approaches to generate partial or whole lung grafts have a great potential not only to resolve current obstacles of lung disease treatments but also to understand disease mechanisms.

The lung is characterized by its complex branching network and massive surface area, tailored to perform efficient gas exchange. Its structure can be divided into three major zones, which are the conducting zone, the transitional zone, and the respiratory zone⁸². The respiratory zone contains alveolar ducts and sacs, where oxygen is exchanged for carbon dioxide. The surface of alveoli is mostly composed of alveolar epithelial type 1 cells (AEC1) and in contact with pulmonary capillaries to allow gas exchange by diffusion. Another important cell type of alveolar is alveolar epithelial type 2 cells (AEC2), which are primary stem cell of the alveolus and responsible for secreting pulmonary surfactant that lines alveoli. Regeneration of distal lung is critical to restore the main function of lung, but it has been challenging due to their size and hollow, complex structures. The diameters of alveoli are ~200–250 μm , and the resolution of most bioprinting techniques is not high

enough to reconstruct the architecture with different cell types at different regions, including surfactant and mucus secretion.

One of the common approaches for lung tissue engineering is the decellularization and recellularization of an existing organ. The biggest advantage of utilizing existing organs is the ability to recreate the intricate lung structure, which is challenging with other currently available technologies. Moreover, decellularized lungs contain ECM including fibronectin, laminin, and collagen type I⁶¹, which are important to support site-specific cell growth. The first lung decellularization/recellularization studies were reported in 2010 by Petersen et al. and Ott et al., in which the regenerated lung was implanted orthotopically and exhibited gas exchange function^{83,84}. To acquire the function of the regenerated lung, appropriate cell population needs to be delivered into corresponding environment. Specifically, recapitulating the alveolar epithelium consisting of AEC1 and AEC2, and reconstructing the vascular network are essential in order to achieve the long-term gas-exchange of the regenerated lung^{85,86}. For the reconstitution of epithelium, carcinomatous human alveolar epithelial cells⁸⁴, human proliferative KRT5⁺TP63⁺ basal epithelial stem cells⁸⁷ and human airway epithelial progenitor cells⁶¹, have been utilized in addition to iPSC-derived epithelial cells^{88,89}. On the other hand, for the re-endothelialization of pulmonary vasculature, primary cells from rat lung microvessels⁸³, rat pulmonary microvascular endothelial progenitor cells⁹⁰, HUVECs⁹¹, and iPSC-derived endothelial cells⁹² have been utilized.

Recellularization is usually conducted via intramural injection of cells or infusion of cells into the vasculature supporting through continuous perfusion⁹³, although the cell distribution is often uneven, and control of the cell placement is challenging due to the complex bronchial tree structure. Additionally, the decellularization process is usually detergent based, which may activate metalloproteinases and then destruct ECM⁹⁴. In addition to various technical difficulties of the decellularization/recellularization process, the obvious drawback is that it relies on the presence of donor organs. However, due to the complicated architecture of the lung, the decellularization-recellularization process currently seems to be the most advanced and promising approach in lung regeneration.

3.1 3D Bioprinting of Lung Tissue

3D Bioprinting of the whole lung is quite challenging due to its complicated anatomy. In order to recreate the blood-air barrier of the lung, the resolution of bioprinting should be as low as submicrons. Using bioprinting techniques at such a high resolution, like laser induced forward transfer, the processing time of a scalable structure would be prolonged. This in turn might reduce the viability of the cells, change the properties of the used material, and increase the risk of machining errors. Moreover, many biomaterials are not suitable for bioprinting of lung scaffolds, as the material needs to have appropriate elastic biomechanical properties required for ventilation cycles during the breathing process⁹⁵. There is always a tradeoff faced by choosing a biomaterial, such as natural biopolymers like alginate⁹⁶, collagen⁹⁷, gelatin⁹⁸, that provide high biocompatibility and biodegradability however they tend to present lower mechanical properties. While synthetic polymers with high mechanical properties lack the ability to promote cell adhesions and biocompatibility⁹⁹. Bioinks based on ECM components, such as proteins derived from decellularized tissues,

also hold the potential to be utilized as bioinks¹⁰⁰. However, enzymatic and decellularization processes lead to the disturbance in the rheological properties that may interfere with their bioprintability¹⁰¹. Therefore, a limited number of studies attempted regeneration of lung utilizing 3D bioprinting. For example, Grigoryan *et al.* generated a vascularized alveolar model utilizing food dyes as photo absorbers for projection stereolithography of poly (ethylene glycol) diacrylate (PEGDA)¹⁰². The generated construct was tested for the oxygenation of human red blood cells during tidal ventilation. Additionally, generation of air-blood barrier model utilizing 3D bioprinting was conducted by Horvath et al., where A549 (alveolar epithelial type II cells; AT-II), EA.hy926 (endothelial) cells were bioprinted layer by layer, while each cell layer was separated by a thin Matrigel layer¹⁰³. Compared to manually seeded constructs, the bioprinted constructs resulted in thinner and more homogeneous cell layers with high reproducibility. However, the constructs were cultured for 3 days only and studying for longer time will be more conclusive. Overall, 3D bioprinting of the whole or partial lung requires a better strategy to reconstitute lung's intricate environment.

Ng et al. built a 3D bioprinted human lung alveolar model using collagen matrix, alveolar lung epithelial cells, endothelial cells, and fibroblasts¹⁰⁴. The cell suspension was modified using 2.5% w/v polyvinylpyrrolidone (PVP), and A549 lung epithelial cells, EA. hy926 human endothelial cells and MRC5 cells were cultured in a hybrid medium of RPMI1640 and DMEM/F12 for seven days, and then bioprinted as top, middle, and bottom layers, respectively. The model was first kept in media for three days and then in ALI for 11 days. High viability (>96%) was observed after 14 days. The study can be used to investigate respiratory-related toxicological studies; however, long-term observation of the developed 3D model is required. A recent study by Kang et al. demonstrated an alveolar barrier by inkjet bioprinting¹⁰⁵. A 3-layered alveolar barrier model was developed from (AEC1) (NCI-H1703), (AEC2), (NCI-H441), and lung fibroblasts (MBC5), lung microvascular endothelial cells along with type 1 collagen. Immunostaining confirmed the presence of tight junction proteins on both sides of the endothelial and epithelial membranes. The presence of adherence junction protein was also confirmed by a high level of mRNA of adherence junction proteins (ZO-1, Occludin). The construct was also tested as a disease model for the influenza virus (H1N1 influenza A), which was applied to the air side of the alveolar barrier model to mimic infection. The model showed a high viral proliferation rate after 24 days, indicating that it can serve pharmaceutical purposes. With the integration of the existing developments in 3D bioprinting, and their application to develop 3D models, can have positive implications for respiratory diseases including severe acute respiratory syndrome-related coronavirus 2 (SARS-CoV-2)¹⁰⁶. Additionally, other appealing 3D bioprinting strategies such as “aspiration-assisted bioprinting (AAB),” which enables picking and bioprinting biologics in 3D using the power of aspiration forces have immense potential to scale up tissue fabrication¹⁰⁷.

3.2. Bioreactors for Lung

Bioreactors are one of the most important components of lung bioengineering. In the past ten years, various applications of bioreactors have been created for lung bioengineering techniques with the goal of creating functional, reproducible tissue constructs. The spectrum

for the lung encompasses entire lung preservation methods through 2-dimensional tissue culture. Especially culture studies with iPSCs are very important for lung bioreactors.

To employ iPSCs for clinical use, a very high cell density is required, which is a tedious process. To circumvent this concern, Rodrigues et al. attempted to develop a cost-efficient way of expanding the number of human-derived iPSCs by dissolvable PGA-based xeno-free microcarriers coated with the xeno-free adhesion substrate Synthemax II to culture iPSC in spinner-flasks¹⁰⁸. They obtained a maximum of 4-fold expansion after 5 days of culture with a ~92% harvesting yield. However, this approach has not yet been used for lung tissue engineering, but more research in this area can prove very promising.

Human-sized ex vivo whole lung bioreactors with perfusion and ventilation that can be automated have been employed for whole lung decellularization and recellularization, as demonstrated by Mortari et al. and Petersen et al. investigated the impact of vascular perfusion pressures on cell survival during 3-day lung cultures in the 10- to 16-mmHg bioreactor^{109,110}. Higher perfusion pressures increased total cell density while vascular perfusion and ventilation decreased cell apoptosis. It was discovered that vascular perfusion alone was insufficient to maintain cultured lung tissue.

Culturing of cell-seeded lungs under mechanical stretch and strain is now possible with the help of ventilation, which can facilitate the differentiation of pulmonary and endothelial cells¹¹¹. Using the same strategy Bonvillain et al., recellularized macaque lung scaffolds¹¹². Taking the approach to human clinical application, Ohata et al. created human-sized lungs from a porcine scaffold lung scaffold. They repopulated it with HUVECs and human basal airway stem cells with the help of ventilation and perfusion⁸⁶.

3.3 Lung-on-a-chip

Microfluidic fabrication technologies have become popular due to their ability to precisely control the environment and to monitor the progress of experiments. As mentioned before, the ability to apply dynamic fluid flow is crucial in recapitulating complex and unique lung environment. Many researchers have focused on establishing the alveolar-capillary or ALI, which is one of the most important features in recreating the lung environment. The pioneering organ-on-a-chip lung model was first created by Zamprogno et al., who have developed a stretchable lung alveoli array with the lung ECM, made of collagen and elastin, populated with primary AEC1 and AEC2, and lung endothelial cells⁷. The size of hexagonal pores of the gold mesh scaffold was 260 μm and cells were cultured at ALI. Huang et al. incorporated alveolar sac-like structure made of gelatin methacryloyl (GelMA) attached to PDMS, which were seeded with primary human alveolar epithelial cells and cultured at ALI while mechanical movement was applied¹¹³. These new generation lung-on-a-chip models can better recapitulate the physiology of alveoli, thus providing better functionality. However, lung-on-a-chip often possesses various cell-to-liquid and surface-to-volume ratios, which are not accurately represented. The surface-to-volume ratio plays a crucial role in autocrine and paracrine signaling¹¹⁴. The secretions and metabolites are diluted because of the volume of the media being larger than the volume of the tissues, which could impact the cells and the effective concentration of drugs available to cells, thus impacting the autocrine/paracrine signaling. Although microfluidic devices are a great way to establish

in vitro models, they lack the complexity of native lung environment and requires further improvements.

Lung-on-a-chip devices have been used in disease modelling studies as well. For example, Huh et al. developed an alveolar-capillary interface model (Fig. 3A) to study the mechanical stress, pathological and physiological activity, toxicity, and absorption of nanoparticulate by the lung¹¹⁵. They developed a lung-on-a-chip model from PDMS (thin, porous, stretchable membrane) and co-cultured epithelial and endothelial cells to form a tight monolayer on each side of the membrane. ALI was introduced by compartmentalization in the microdevice, and the alveolar air space lining was mimicked by introducing air in the epithelial compartment. They used the model to mimic innate immune response to bacterial pulmonary infections. The presence of GFP-tagged *E. coli* on the apical surface of the alveolar epithelium for 5 h activated the endothelium to produce neutrophils that were found circulating in the microchannel, displaying a directional movement for their phagocytic activity toward *E. coli*. The study also revealed the mechanical stress-induced nanotoxicity in lungs, quantified by the amount of reactive oxygen species (ROS) production. 12 nm silica nanoparticles in the alveolar epithelium and cyclic strain (10% at 0.2 Hz) increased the ROS production by a factor of 4 within 2 h. The same response was also observed in the endothelial layer, though the response was delayed by an hour compared to the epithelial layer. Although the model can help in low-cost screening, it does not satisfy the required barrier thickness. As a follow-up study, Stucki et al. developed a lung-on-a-chip model (Fig. 3B) in PDMS (thin, porous, stretchable membrane) and co-cultured epithelial and endothelial cells to form a tight monolayer on each side of the membrane¹¹⁶. They used primary human pulmonary alveolar epithelial cells (HPAECs) from lung resection from cancer patients undergoing pneumonectomy. To mimic the alveolar sac environment, epithelial cells on the apical end and HUVECs were seeded on the basal end of the PDMS membrane. They created an air-blood barrier of 1–2 μm and induced the mechanical stress experienced during breathing movements using a micro-diaphragm. A breathing rate of 12 cycles per min was used to create a strain that led to 10% elongation in the model. The results showed that initially, no interference was seen with the activity of HPAEC, but after 48 h of strain, metabolic activity was significantly higher than in static cells; along with this, the IL-8 production was also 2.5 times higher when kept under 48 h of stretching than those in the static state.

Organ-on-chip platforms offer a novel and distinctive technologies for research on a variety of diseases by advancing methods for both diagnosis and therapy, which are crucial areas of study for enhancing global health. Such platforms' main drivers are the removal of in vivo animal testing and the time and money savings in drug development. Organ-on-chip research has advanced significantly and has several unique characteristics. These include the capacity to apply mechanobiological stimuli, facilitating 3D cultures and cell-cell interactions, online testing monitoring, and affordable testing¹¹⁷. Several obstacles still need to be addressed, and the full potential has yet to be realized^{118,119}. Most chips are manufactured from PDMS because of its usability, excellent optical clarity, gas permeability, and biocompatibility. PDMS has a high solubility in nonpolar organic solvents because it is hydrophobic, which causes the polymer to swell¹²⁰. The exploration of surface modification techniques, such as coating with glass¹²¹ and metal oxides¹²² as well as replacing PDMS entirely with

fluorinated compounds¹²³, has been prompted by interest in the use of microchannels for organic reactions. The goal is to decrease the absorption of organic solvents into the polymer bulk.

Due to a variety of appealing features, PDMS has been proven to be essential to the development of microfluidics platforms during the past fifteen years. However, a few drawbacks have been mentioned that cast doubt on the use of PDMS as a medium for cell-based investigations. Deformation, evaporation, absorption, leaching of uncrosslinked oligomers, and hydrophobic recovery are some of the drawbacks of PDMS that might be problematic for microscale cell research¹²⁴. Remaining uncrosslinked polymer chains in cured PDMS can easily disperse throughout the bulk material. These uncrosslinked oligomers may diffuse out of the bulk matrix and into the solution when in contact with the solution. According to Regehr et al., uncrosslinked oligomers were shown to leak. To be able to integrate into cell membranes when studied in cell culture, they demonstrated that PDMS dramatically reduced estrogen levels in the culture medium, inhibiting activator protein-1 activation via estrogen signaling, demonstrating the biological impact of small molecule absorption¹²³.

Although PDMS provides elastic and biocompatibility properties, its synthetic nature has a distorted biochemical microenvironment and different molecular composition from ECM. This leads to an emerging need for a new type of material that can be used for organ-on-a-chip models. Zamprogno et al. developed a second-generation lung-on-a-chip model, replacing PDMS with another stretchable biological material, a soft collagen-elastin (CE) membrane developed by Dunphy et al. The membrane had the same protein composition as ECM and can be used for the air-blood barrier^{7,125}. They used a gold mesh with a pore size of 260 μm as the scaffold, supporting 40 arrays of alveoli. CE was drop cast on the gold mesh. The membrane was used to coculture primary HPAECs with primary human lung endothelial cells. This study demonstrated that the CE membrane absorbs 90% less Rhodamine B when incubated with 10 μM of Rhodamine B for 2 h compared to the PDMS-based membrane. Along with more deflection in CE membrane compared to PDMS, there was no need for preliminary coating in CE membrane for cell culturing, contrary to fibronectin coating required for PDMS. Due to the above advantages, CE-based membrane can be used in organ-on-a-chip models for more advancement in pulmonary research.

A widely used quantitative method for assessing the integrity of tight junction dynamics in endothelial and epithelial monolayer cell culture models is transepithelial/transendothelial electrical resistance (TEER). It is based on measuring ohmic resistance or impedance across a broad frequency range and can be carried out in real-time without causing cell damage¹²⁶. Harrington et al. used epithelial cells, fibroblasts, and dendritic cells cultured on scaffolds to create a 3D in vitro model of human upper airways. The model's peak TEER value of 200 $\Omega\cdot\text{cm}^2$ was comparable to 260–320 $\Omega\cdot\text{cm}^2$ TEER measurement of rabbit airway epithelium¹²⁷. Several, stable and viable microfluidic in vitro epithelial models have been developed consisting of A549 cells cultured under an ALI with TEER values ranging from 120 to 195 $\Omega\cdot\text{cm}^2$ ¹²⁸. So far, none of the microfluidic systems that were built to determine pulmonary function have embedded electrodes to acquire real-time TEER measurements. The intricate morphology and physiological processes of the lung may be

accurately modeled in vitro, which would be a very useful tool for drug development. An in vitro model representing the complex morphology and physiological functions of the lung with the inclusion of electrodes for on-chip measurement can be a big step forward for next generation models/chips systems.

3.4 Organoids

Recapitulating the lung environment has also been attempted by growing lung organoids. Organoids, which are stem cell derived self-organizing structures, are promising in establishing cell-cell and cell-ECM interactions. Many different studies have successfully generated organoids from different types of lung cells. For example, organoids derived from alveolar epithelial cells are called “alveolosphere¹²⁹”, ones from trachea basal cells are called “tracheospheres¹³⁰”, and ones from bronchi or large airways are called “bronchospheres¹³⁰”.

Human iPSC derived organoids are popular in establishing lung organoids. Chen et al. developed lung bud organoids with branching airway and early alveolar structures. The branching structures were shown to reach the second trimester of human gestation¹³¹. Jacob et al. established a differentiation protocol to generate AEC2 from iPSCs. The differentiated cells exhibit AEC2 functions, such as the production of lamellar bodies, and can form alveolospheres in 3D without mesenchymal feeders, which are required to maintain the AEC2 phenotype when isolated from primary tissue¹³².

Many studies also generated lung organoids from primary tissues. From broncho-alveolar resections or lavage, Sachs et al. produced human airway organoids consisting of basal cells, functional multi-ciliated cells, mucus producing secretory cells, and club cells¹³³. Tindle et al. generated human lung organoids from primary lung tissue, which contain both proximal and distal airway epithelia¹³⁴. 2D Monolayer culture containing both proximodistal airway cells was tested for SARS-CoV-2 viral infection, in which proximal airway cells were shown to be susceptible for infection while distal alveolar cells were responsible for host response. Utilizing organoids for viral infection studies may be challenging since many lung organoids contain apical-in architecture. In most cases, organoids are dissociated into single cell suspension and cultured in 2D monolayer, which might result in the loss of the organoid structural integrity¹³⁴. Therefore, generating apical-out polarity lung organoids have been accomplished to facilitate more effective infections. Apical-out airway organoids were produced from 2D-expanded bronchial epithelial cells and differentiated in suspension to produce uniformly-sized organoid cultures with strong ciliogenesis in an ECM-free environment. The difficulties that ECM-embedded airway organoids face can be solved using micropatterned plates followed by suspension culture. This may also enable the use of apical-out and high-throughput tests like antiviral drug screening¹³⁵.

Primary stem cell-derived organoids rely on the supply of primary tissues but are useful in modeling rare diseases. On the other hand, iPSC-derived organoids can be genetically modified via CRISPR/Cas9, which enable studying diverse types of lung diseases, but they tend to have difficulties to mature up to adult-like stage¹³⁶. Since many lung organoids are composed of epithelial cells, introducing non-epithelial cells would be better in recreating native-like structures in the future.

4. Airway Tissue Engineering

The majority of studies pertaining alveolar models has focused on simulating the interactions between the air, cells, and fluid. With the use of “organ-on-a-chip” technology, this engineering has advanced significantly. One of the earliest breathing alveolar models was developed by Huh et al. outlined a computerized air-liquid two-phase microfluidics-integrated airway system that enabled accurate simulation of physiological or pathologic liquid plug flows seen in the respiratory system as well as on-chip fabrication of human airway epithelia¹³⁷. They demonstrated cellular-level lung damage with apparatus under flow circumstances that resulted in symptoms typical of a variety of pulmonary illnesses. Park et al. employed 3D printing to form a model of an airway-on-a-chip. A naturally derived blood vessel network was formed in vitro using ECM from porcine tracheal mucosa (tmdECM) for hydrogel encapsulating human dermal epithelial cells and human lung fibroblasts on a PCL frame⁹⁶. tmdECM derived endothelial cell re-orientation that led to blood vessel and lumen formation. The model was used for disease modeling for asthmatic airway inflammation and allergy-induced asthma. In a recent study, Si et al. formed a microfluidic bronchial airway-on-a-chip to construct a model for viral infections⁶³. Primary human lung airway basal stem cells were cultured under ALI on one side, while primary human lung endothelium was cultured on the opposite side. Airway-specific cells were formed on the microfluidic chip, including mucociliated, goblet cells, club cells, and basal cells. Along with this, formation of ZO-1 and cilia was also formed, and a similar permeability barrier and mucous production were observed. It also served as a model for influenza virus infection and testing for the efficacy of antiviral therapeutics. Additionally, the model also served as a platform for SARS-CoV2 by introducing pseudo particles containing SARS-CoV-2 spike (S) protein onto luciferase reporter gene carrying retroviral core particles. Viral pol gene encoded by SARS-CoV-2pp detected in lung airway epithelial indicating its potential for preclinical studies of the prospective drugs in viral lung infections.

5. Disease Models

Respiratory diseases, such as chronic obstructive pulmonary disease (COPD), asthma, idiopathic pulmonary fibrosis (IPF), tuberculosis, and lung cancer cause significant morbidity and mortality globally and have a daily influence on the lives of millions of people¹³⁸. Unfortunately, many of these chronic pulmonary diseases are considered irreversible and progressive resulting in increased premature deaths. In addition, due to minimal regeneration capabilities, the only option to restore permanently damaged and defective airways is through transplantation, which is majorly challenged by the limited donor availability¹³⁹. A successful tissue engineering approach can also provide physiologically-relevant lung disease models. Animal models or human pathology specimens have formed the basis for our understanding of the pathogenesis of several diseases; however, increasing number of in-vitro models using human cells have been developed and used for modeling several pathologies¹⁴⁰ including lung diseases¹⁴¹.

5.1 In-vitro Disease Models

Human iPSC-derived models of pulmonary diseases have potential for recapitulating the course of hereditary disorders, for which only end-stage samples are often available. Large quantities of lung cells with disease phenotypes and control populations may potentially be made available for toxicity research and the development of new treatments. Lung cells produced from human iPSCs have previously been used in proof-of-concept modeling of pulmonary diseases. The earliest studies of lung lineage differentiation from iPSCs occurred in a 2D setting and produced progenitor cells that were similar to those that were stimulated early on during lung development in the embryo¹⁴². They established culture conditions that enabled numerous cells (ESC-derived Nkx2-1⁺ lung progenitors, Nkx2-1⁺ endodermal progenitors) in culture to stochastically develop into lung epithelium-specific cell types, including those from both the airway and alveoli, to mature these iPSC-derived progenitors. The study of hereditary lung disorders, especially cystic fibrosis (CF), has benefited from the use of patient-specific iPSCs. Recently, mature lung cells from CF-iPSCs were produced¹⁴³. To demonstrate that genome engineering techniques can be used for functional gene correction to the Cystic Fibrosis Transmembrane Conductance Regulator (CFTR) in a patient-specific manner, researchers have used CF patient-specific iPSC-derived lung cells¹⁴⁴. This work may pave the way for the use of these systems in identifying novel therapeutic strategies. The advantages of iPSCs are their endless supply and simplicity in genetic modification. Human iPSC differentiation is still being optimized for the creation of pure populations of mature cells and requires ongoing validation against human lung samples, much as the human embryonic lung cells generated in vitro. These in vitro methods are all adaptable for disease modeling and testing regeneration therapies, and they are mostly complimentary. Collaborations with bioengineers to incorporate more physiological elements like ventilation, gas concentrations, and ECM are anticipated to lead to further advancements in these models^{145,146}.

Huh et al. used soft lithography-based microfabrication methods to create a lung-on-a-chip model made of PDMS that could mimic the human alveolar-capillary interface, and also the mechanical strain caused during breathing¹⁴⁷. To reconstitute the alveolar-capillary interface of the human lung, alveolar epithelial cells made up the upper side of the ECM covered porous membrane, while lung capillary endothelial cells made up the lower side. The developed device mimicked physiological organ-level functions. The model was able to mimic the lung inflammation, which was confirmed by transmigration of neutrophils and pro-inflammatory cytokines. Along with it, the device was able to replicate the innate immune response against microbial lung infections that was caused by GFP labelled *E. coli* bacteria. In addition to this, the model was also used to study the toxicology caused by silica nanoparticles that resulted in acute lung inflammation. Another microfluidic lung model with an airway of epithelial cells was created by Sellgren et al. where lung fibroblasts and microvascular endothelial cells were cultivated over an ALI culture in three compartments that each were vertically stacked and divided by a nano porous membrane¹⁴⁸. A reversibly bonded alveolus-on-a-chip model was developed by Stucki et al. to replicate the pulmonary parenchyma's milieu¹¹⁶. They stretched the alveolar barrier with a micro-diaphragm to mimic the in-vivo diaphragm. Benam et al. stimulated tiny airway chips lined by either normal or chronic obstructive pulmonary disease (COPD) epithelial cells with

the viral mimic polyinosinic-polycytidylic acid (poly(I:C)) or with lipopolysaccharide (LPS) endotoxin, a component obtained from bacterial walls that increases cytokine production¹⁴⁹. Nesmith et al. created an anisotropic, laminar bronchial smooth muscle tissue on elastomeric thin films that replicates normal and asthmatic bronchoconstriction and bronchodilation in vitro¹⁵⁰. The muscle layer constricted and caused thin film bending in response to a cholinergic agonist, acting as an in vitro model of bronchoconstriction. They subjected the modified tissues to interleukin-13 (IL-13), which led to hypercontractility and abnormal relaxation in response to cholinergic stress. These effects were comparable to those shown in investigations with animal tissue and in the clinical trials of asthmatic patients. A muscarinic antagonist and a beta-agonist, which are used clinically to relax constricted airways, were also used to reverse asthmatic hypercontraction. In another study, Huh et al. created a disease model of pulmonary edema in human lungs using a lung-on-a-chip device¹¹⁹. Pulmonary edema is a potentially fatal condition marked by abnormal accumulation of intravascular fluid in the interstitial tissues and alveolar air spaces of the lung because of impaired homeostatic fluid balance mechanisms that cause vascular leakage across the alveolar-capillary barrier¹⁵¹. They used optically transparent silicone elastomer, which has two parallel microchannels separated by a thin, porous, flexible membrane coated with ECM, and two layers of human alveolar epithelial and pulmonary microvascular endothelial cells grown near one another. Culture media was fed through the microvascular channel and the alveolar epithelium was exposed to air to simulate the alveolar/air gap, and cyclic vacuum was delivered to hollow side chambers to cyclically stretch the tissue layers and replicate physiological breathing motions.

Jain et al. modified a previously described lung-on-a-chip device (Fig 4A), which consists of two parallel rectangular microchannels separated by a thin, porous, flexible membrane coated with ECM, to create an organ-level model of vascular inflammation-induced human pulmonary thrombosis that is also capable of dissecting intercellular communication¹⁵². HUVECs were lined up inside the bottom microchannel to create a micro-vessel that prevents blood from contacting the prothrombotic ECM-coated channel walls as occurs in native blood vessels. They were able to build a 3D cross-section of a human lung alveolus with an alveolar-capillary interface and a vascular lumen that allows for the perfusion. Tavana et al. provided details of a microfluidic device that was inspired by pulmonary airways and allows for the on-chip production of liquid plugs that block airways from a stratified air-liquid two-phase flow¹⁵³. This platform holds the potential to perform systematic investigation of the effect of different degrees of fluid mechanical stresses on lung injury. Hassel et al. developed a chip that enables the development of a model of non-small-cell lung cancer that simulates tumor dormancy and tumor growth unique to the organ microenvironment, and responses to tyrosine kinase inhibitor (TKI) treatment seen in human patients in vivo¹⁵⁴. Felder et al. demonstrated an in-vitro microfluidic wounding model to replicate alveolar epithelial microinjuries¹⁵⁵. The first phase involves reproducing epithelial lesions with dimensions that correspond to the human alveolus. Most recently, techniques of tissue engineering have been explored to provide better models of airway physiology¹⁵⁶. To explore cell-cell interactions and remodeling, a human bronchiole model was created, consisting of cylindrical bronchioles made from human lung primary cells, lung fibroblasts, airway smooth muscle cells, and ECM¹⁵⁷. The designed bronchiole's cylindrical

form causes the tissue to apply radial stress, which indicates mechanotransduction, and the air rushing through the lumen creates a natural environment for the epithelial cells. Research on specific aspects of airway remodeling, such as subepithelial fibrosis, smooth muscle hyperplasia and hypertrophy, and epithelial cell metaplasia, may be performed using this created model of the bronchiole.

Cell-ECM interactions, interactions with other cell types, and exposure to growth factor gradients occur while cells are submerged in a 3D environment *in vivo*¹⁵⁸. As opposed to what is often observed in 2D, fibroblasts exhibit distinct integrin adhesions in 3D¹⁵⁹. Bronchial epithelial cells developed into polarized acini and endothelial cells exhibit greater sprouting angiogenesis¹⁶⁰. Using a 3D dynamic construct that allows for cell migration, traction, and integrin adhesion; lung-on-a-chip models aim to mimic the native tissue conditions, with improved cell-cell and cell-matrix interactions. By developing a facile and more reproducible approach using a decellularized ECM (dECM) based bioink, Park et al. developed a vascular platform by direct 3D bioprinting of cell-laden dECM bioinks, then investigated its function upon integration with the airway epithelium model⁹⁶. The model presented respiratory disease symptoms, including asthmatic airway inflammation and allergen-induced asthma flare-up, in physiological context. A microscale organotypic model of the human bronchiole for studying pulmonary infection featuring a triculture system of the human bronchiole was shown to be feasible by Barkal et al.¹⁶¹. The model consisted of three cell-lined (epithelial cell-lined lumen and endothelial cell-lined lumens) within a 3D matrix of collagen and pulmonary fibroblasts. To mimic the airway, the central lumen was lined up with primary human bronchial epithelial cells while the two flanking lumens form the vascular compartment and were lined up with primary human lung microvascular cells. Results indicated that the organotypic bronchiole model and microbial volatile extension can potentially be used to investigate the initial events in the host response to respiratory pathogens.

5.2 Preclinical/Clinical Testing of 3D Printed Grafts

The use of 3D printing to address clinical issues in pulmonology has recently been described by several groups. Using CT scan data, Morrison et al. produced customized airway splints for children with tracheobronchomalacia¹⁶². Under the medical device emergency use exemption, airway splints were implanted. All patients had the anticipated responses to the treatment. There are increasing number of case reports describing the use of 3D printed models for planning thoracic surgery or stent implantation. To better identify and define the degree and location of stenosis or malacic alterations, Tam et al. 3D printed an airway model using a CT image from a patient with tracheobronchial chondromalacia¹⁶³. To facilitate surgical planning, Kurenov et al. demonstrated that it is simple to 3D print pulmonary arteries using CT data¹⁶⁴. The usefulness of their 3D printed bioresorbable external airway splint in prolonging life in a pig model of severe tracheomalacia was also demonstrated later¹⁶⁵. An extraluminal excision of a tracheal ring, subperichondrial separation of the internal tracheal mucosa, and division of the overlaying tracheal rings were used to construct a surgical model of tracheomalacia in 2-month-old Yorkshire piglets. In an adult patient with secondary tracheomalacia brought on by endobronchial tuberculosis, Huang et al. describe the first application of a 3D printed bioresorbable external airway

splint¹⁶⁶. The scaffold was surrounded with an artificial pleural patch to stop erosion into the neighboring buildings. These studies have demonstrated the viability, efficacy, and safety of 3D printing external airway splints for tracheobronchomalacia. However, prior to testing a 3D printed system in a pre-clinical model or human being, we must be sure that the engineered system matches the design inputs. To demonstrate the execution of modular scaffold engineering based on 3D printing for clinical translation within the design control framework, Hollister et al. developed a tracheobronchial splint to meet the quantitative design inputs using image-based topology design techniques followed by laser sintering of PCL¹⁶⁷. Les et al. demonstrated the initial clinical efficacy in 15 young patients with severe tracheobronchomalacia successfully receiving 3D printed, bioresorbable patient-specific splints on their trachea using this design¹⁶⁸. Huh et al. demonstrated the proof of concept for a human disease model that simulates pulmonary edema utilizing a biomimetic device that mimics organ-level lung functions (Fig. 4B). The microfluidic device, which recreates the alveolar-capillary interface of the human lung, was made up of channels lined up by layers of human pulmonary epithelial and endothelial cells that were closely apposed and experience fluid and air flow as well as cyclic mechanical strain to imitate breathing motions¹⁶⁹.

5.3 In-silico Disease Models

Computational or in-silico techniques are other methodologies to model human lung disease. The in-silico models make use of data from in vitro and in vivo models and apply computational algorithms to incorporate a variety of physiological characteristics that may have an impact on drug deposition and distribution. In-silico modeling of airway mechanics, airflow dynamics, and particle deposition in lungs could provide better understanding into toxic inhalation, the spread of infectious lung diseases, and drug delivery. Martonen et al. proposed a mathematical model with the intention of exploring the various factors influencing particle deposition in disease-induced lung model to investigate the alterations in particle behavior in an asthmatic lung¹⁷⁰. Nowak et al. predicted the particle deposition in the whole lung using computational fluid dynamics¹⁷¹. According to the authors, changes in aerosol deposition into the lungs caused by intersubjective variability were primarily seen in the proximal airways and were barely noticeable in the deep lung. However, the study did not take into consideration the upper airways. Later, Annapragada & Mishchiy reported an accurate and comprehensive model of the aerosol deposition in human lung by combining a computational fluid dynamic (CFD) (Fig. 5A) for the proximal airways and an analytical or semiempirical computational model for the deep lung¹⁷². Based on the morphological and geometrical data gathered by medical imaging on healthy human participants, Ma et al. created a human airway model stretching from the mouth up to generation 10 of the tracheobronchial tree¹⁷³. The results showed that the computed extra thoracic deposition, the ratio of the amount of aerosol deposited in each lung and the efficiency of deposition at the generational level correlated with the in vivo and in vitro data available and that the majority of the micrometer-sized aerosol particles were deposited in the large-medium airways.

Furthermore, it is crucial to comprehend and estimate particle movement and deposition in the alveolar region while designing an aerosol-based delivery system. 3D Structure of acinar airways, alveolar geometries and airflow are likely to have a considerable impact on particle

deposition in this area. Among a variety of different possible shapes, Hansen et al. identified the 3/4 spheroid as the most typical shape of an alveolus¹⁷⁴. During breathing, the shape and size of airways continuously alter in an acinar region, affecting the particle transport by changing the pattern of airflow. Therefore, in order to simulate acinar airways accurately and estimate the aerosol deposition, it appears essential to include moving wall and ventilation aspects¹⁷⁵. The work of Koshiyama & Wada, initially validated using rodents, led to the development of a realistic in-silico human acinar airway models (Fig. 5B) where the algorithm generated heterogeneous acinar structures made up of irregularly sized alveolar cavities assembled into a complexly branched, space-filling ductal tree that captures the morphometrical characteristics of the acinus, including local acinar heterogeneity¹⁷⁶.

CFD provides an in-silico method to evaluate the performance of a device holistically, from calculations of medication dispersion to lung delivery efficiency. Towards complete-lung simulations, Koullapis et al. presented a numerical methodology to forecast particle deposition in a simplified approximation of the deep lung during a whole breathing cycle, with an eye toward large-scale simulations of the human lung¹⁷⁷. The geometrical model used comprises of a space-filling algorithm-created heterogeneous acinar model and an idealized bronchial tree that represents generations 10 to 19 of the conducting zone. The authors demonstrated resulting deposition to agree with classic deposition predictions with significant computational cost savings were achieved by simulating airflow and particle movement in a single representative bifurcation and a single acinar model. Recently, Poorbahrami et al. reported a whole lung in-silico model to estimate age dependent particle dosimetry in the newborn, child, and adult subjects¹⁷⁸. This was performed by coupled simulations that included CT-based airway geometry, accurate respiratory wave forms, and realistic particle diameters (1, 3, and 5 μm). The results illustrate regional disparities at both the lobar and regional (conducting versus respiratory) levels. Overall, taking into consideration the genetic variety in human populations, in-silico approaches may complement some of the advanced methodologies of in vitro organ-on-a-chip platforms in drug discovery to predict toxicology and further model lung diseases.

6. Clinical Translatability

The past decade has seen significant progress in the development of technologies that can improve our understanding during the early stages of lung diseases. The development of 2D and 3D culture systems that more closely resemble the physiological characteristics of native tissues than conventional plate culture methods or even animal models is one of these emerging technologies¹⁷⁹. These models allow us to study adverse drug reactions, prospective pulmonary problems like drug-induced angioedema, or even responsiveness of medications well before the start of clinical trials by simulating human disease states and pathologic pathways of drug-induced lung diseases. Most of the current treatment strategies and medication for pulmonary diseases serve to delay the progression and not as curative treatment. Various models have been developed over time to explore lung physiological responses and pathological changes in lung diseases. The distinctions between models depend on the medical condition being examined and what part of the lungs the built system is trying to emulate. These models allow us to explore the molecular mechanisms of healthy

and diseased conditions, lung progenitor cell responses, crucial cues in lung formation, or reactions of respiratory tissues to ECM and mechanical stimuli.

The development and successful transplantation of patient-specific engineered whole lungs is very challenging and may require more technical advancements. The first lung transplantation in a human was performed 1963¹⁸⁰. Although the patient died of renal failure post 18 days of transplantation, the lung was demonstrated to have functioned with only minor evidence of rejection. Since then, multiple attempts at lung transplantation have failed mainly due to rejection and problems with anastomotic bronchial healing. With the advancements in surgical settings over the years such as the invention of the heart-lung machine, coupled with the development of immunosuppressive drugs, lungs could be transplanted with a higher chance of patient recovery. The world's first successful heart-lung transplant was performed in 1981 on a 45-year-old woman with primary pulmonary hypertension¹⁸¹. In 2021, a team of Mount Sinai, New York surgeons has performed the world's first human tracheal transplant in a 56-year-old female patient. The patient has had no complications or signs of organ rejection and doctors are monitoring her closely to assess her progress and reaction to antirejection therapy¹⁸². Although this protocol is not involving any "tissue-engineered" trachea, rather donor trachea only, this procedure has the potential to save the lives of thousands of patients around the world, who have tracheal birth defects, untreatable airway diseases, or severe tracheal damage from intubation.

For reconstruction of segmental tracheal defects, Delaere et al. reported a successful allotransplantation of a pre-vascularized tracheal graft via transplantation of the graft over the patient's left forearm's dissected subcutaneous tissue¹⁸³. On Day 34 after implantation, the patient's buccal mucosa was placed on the posterior tracheal wall, resulting in a chimeric epithelial lining four months later. Despite this, after stopping immunosuppressive therapy prior to orthotopic tracheal transplantation, the donor endothelial and respiratory cells vanished. After the transplant, the patient's pulmonary function improved. A tissue engineering strategy was used to carry out bronchoscopic lung volume reduction, a surgery intended to improve the respiratory function in patients with severe emphysema. The study used a fibrin sealant to encourage the creation of scar tissue and the subsequent resizing of the lung improved respiratory performance without causing the severe trauma often connected with surgery¹⁸⁴. Elliot et al. reported a two-year follow-up on a 10-year-old boy, who was born with segmental congenital tracheal stenosis and pulmonary sling⁵⁹. A tissue-engineered trachea was transplanted in 2012. The decellularized cadaveric donor trachea was seeded with unexpanded autologous BM-MSCs and epithelial patches. One week after the operation, there was evidence of revascularization, and in the first eight weeks, there was a strong neutrophil response. However, the graft did not have biomechanical strength focally until 18 months post-surgery. A 2-year follow-up showed that the patient had a functional airway. The same work was continued by Hamilton et al. for a 4-year follow-up study in the patient¹⁸⁵. Biopsy of the transplanted trachea showed complete epithelial layer having squamoid and respiratory type epithelium along with some ciliated cells when observed 42 months after the surgery. Along with the longest follow-up study, this research was also the first that has used CFD simulations to provide the information on pressure within the reconstructed trachea.

After the success of above-mentioned tissue-engineered tracheal grafts, the same group of scientists prepared another tracheal graft using the same technique for a 15-year-old girl suffering from critical tracheal stenosis¹⁸⁶. Autologous BM-MSCs and nasal-derived epithelial cells were used for seeding a decellularized cadaveric trachea in an ex vivo bioreactor. 15 Days post-surgery, the clinicians suspected a possible acute extrinsic compressive event that led to airway obstruction and resulted in her death. This imposed a question on insufficient preclinical validation of the safety of the used technique, the clinical protocols used for transplantation and the continuous need to improve the preclinical studies. The team also proposed to use indwelling stents for several months after implantation to improve future outcomes. Pepper et al. studied the performance of tissue-engineered trachea made of a synthetic scaffold in an ovine model⁷⁹. 20% polyethylene terephthalate (PET) and 80% polyurethane (PU) polymer nanofiber precursor solutions were blended using electrospinning and were further reinforced with polycarbonate rings. The scaffolds were seeded with autologous bone marrow derived mononuclear cells and implanted in juvenile sheep. Results showed neovascularization at the anastomosis site, but no epithelialization was found after necropsy. Along with this sign of infection, inflammation was always seen in the native airway epithelium. Therefore, further preclinical studies are needed to prevent the host response upon implantation. To achieve a high regenerative capacity of the trachea, Kim et al. used iPSC-derived cells to construct a novel two-layered tubular scaffold as a tracheal graft¹⁸⁷. The trachea was reconstructed using a bioreactor, and the graft was implanted in a rabbit model. The results showed epithelium formation with no evidence of infection. Tensile strength was also shown to be similar to the native trachea. Although native trachea was found at distal sites, iPSCs-derived cells could not replace the cartilage on the native trachea. That study opens the possibility of using iPSCs-derived cells for tracheal reconstruction; however, further studies in larger animals are required to validate the results.

Chronic pulmonary diseases, including idiopathic pulmonary fibrosis (IPF), pulmonary hypertension (PH), and chronic obstructive pulmonary disease (COPD), are cause of high morbidity and mortality worldwide and have limited clinical management options available¹⁸⁸. Pulmonary fibrosis refers to a group of lung conditions marked by the formation of scar tissue and idiopathic pulmonary fibrosis (IPF). Pirfenidone and nintedanib were approved by the American Food and Drug Administration (FDA) in 2014 to slow the progression of IPF's functional loss^{189,190}. However, many other drug targets failed phase II/III human clinical trials mainly due to the fact that current animal models of pulmonary fibrosis (e.g. bleomycin) do not accurately mimic human IPF condition¹⁹¹. Sava et al. used decellularized IPF ECM to functionalize polyacrylamide hydrogels to decouple biological reactions from matrix mechanics¹⁹². In response to increases in local substrate stiffness, human microvascular pericytes grown on these human lung ECM-conjugated hydrogels with tunable mechanical properties underwent phenotypic transition measured by expression of smooth muscle actin (SMA), independent of receptor-ligand interactions with IPF ECM. Additionally, the tyrosine-kinase inhibitor Nintedanib, which is approved for the treatment of IPF, decreased the expression of SMA and the detection of crosslinked collagen by pericytes. COPD is another condition that results in a progressive loss of lung function, leading to respiratory failure. Shronska-Wasek et al. reported an ex vivo 3D lung tissue

culture (lung slices) that decreased frizzled receptor 4 expression in COPD inhibits WNT/-catenin-driven alveolar lung regeneration¹⁹³. Although these models show promise for drug discovery and preclinical testing of airway remodeling in COPD, they have significant limitations due to their low post-dissection viability, low preservation of vital structural integrity, and degraded cell-cell and cell-matrix interactions in longer-term experiments. The preclinical and clinical studies are often needed for ensuring safety and effectiveness of new approaches and they enable better research and understanding with best cost-benefit ratios. Although most of the pre-clinical trials are yet to be translated into clinical trials, the results from several bioengineering strategies are promising for future clinical applications. Currently, several clinical trials can be identified in the [ClinicalTrials.gov](https://clinicaltrials.gov) database when using the keywords “Lung Diseases” and “Bioengineering” (Table 1), from which 5 are active and recruiting. This indicates ongoing dynamic research and product translatability in the field towards better lung healthcare.

Additive manufacturing strategies such as bioprinting have immense potential for clinical translatability of autologous, vascularized, functional, ethically feasible and scalable constructs¹⁹⁴. Concurrently, organ-on-chip technologies have a great deal of promise for enhancing the preclinical to clinical translation of medication research¹⁹⁵. The use of organ-on-a-chip technologies to replace animal testing for preclinical medication efficacy and safety is receiving more attention¹⁹⁶. Although animal models can offer a complete in-vivo testing platform for pharmaceuticals, their drawbacks, particularly inter-species variances, make it challenging to anticipate how well an animal model would translate to humans. The creation of patient-derived organoids and organ-on-chip models made up of patient-derived cells are two methods that are more relevant to humans. For example, Benam et al. developed a human lung small airway-on-a-chip model containing primary airway epithelium from COPD patients to show different cytokine release profiles in response to inflammatory stimuli and cigarette smoke and used controlled levels of IL-13 in healthy chips to induce aspects seen in asthma, such as increased inflammatory response¹⁴⁹. Additionally, lung-on-a-chip models can achieve some level of personalization using patient samples or biomarker levels typically seen in diseased patients. Although regulated integration of a decellularized ECM hydrogel has been promising for “personalizing” lung-on-a-chip models, other patient samples, such as the use of iPSCs or patient-specific ECMs, have not been incorporated yet⁹⁶. Aiming to evaluate the robustness, repeatability, and dependability of various organ-on-chip platforms as well as the difficulties in transferring organ-on-chip systems from bench to bedside, new research centers have been established in the US. Additionally, the US National Institutes of Health support the micro-physiological systems database, a source of technical, analytical, and biological information can be utilized to develop guidelines for organ-on-chip validation. Future advances in precision medicine may be made possible by multi-organ interactions, in which several organs-on-chips are linked together in a network to characterize tissue responses more thoroughly.

7. Conclusion and future perspectives

This review offers an overview of the recent developments in tracheal and lung tissue engineering particularly with respect to 3D printing, bioprinting, bioreactors, organoids, and organ-on-a-chip technologies. The development of these advanced technologies has

the potential to transform the field of medical sciences by fabricating superior scaffolds for regenerative medicine and tissue and organ transplantation, and physiologically-relevant organ-on-a-chip platforms for drug testing and disease modelling. The lung is a complex organ with high potential to environmental or systemic harm, which only advances with aging. The repair and regeneration of damaged lung has been the subject of several preclinical animal research; however, they have not yet been translated into human clinical trials yet. Cell-based therapeutics stimulating endogenous stem/progenitor cells or providing with exogenous factors have seen some success. However, in cases where lung repair is no longer an option, a tissue-engineered lung using decellularized ECM or bioengineered scaffolds are a viable alternative. Decellularized lung ECM appears to be the most promising scaffold for whole lung regeneration while artificial biomatrix constructs could be used for the larger single airways. Being a complex organ, there are multiple cell types across the pulmonary vasculature, airways, and lung parenchyma. The use of iPSCs may allow for diminished to absent immunogenicity with sufficient cell quantities. One of the challenges is to mimic the native architecture of the lung, where each capillary is surrounded on both sides by a cell-thick epithelium, needed to maximize efficiency of gas exchange. Regulation and understanding of angiogenesis to create intricate pulmonary vasculature might help overcome this limitation. Strategies employing ex vivo lung perfused systems and human-sized bioreactors are now within reach for the decellularization and recellularization of lung.

Bioprinting may provide the technological advancement required to translate biological grafts via rapid manufacturing of tissues tailored to individual patients at a clinical scale. Requirements include appropriate cell sources for the tissues from the ciliated epithelium through the alveolar epithelium in each layer and creation of the airways. This could be made possible using host-iPSCs. Additionally, it is essential to maintain the lumen patency of the lung along with vasculature; and the formation of alveoli requires a sealed air/fluid interface using numerous cell types intimately related with convoluting microvessels. For optimal results, the bioprinted lung will also require to be integrated with a dynamic bioreactor that can ventilate the tissue while supplying nutrients and gaseous exchange. Recently, the development of “organ-on-chip” technology has the potential to expedite research targeted at unraveling the intricate biology of lung illnesses as well as speed up the drug development. The aim is to fill the gap between effective drug identification and disease, drug research while encouraging in vitro investigation into complex systems in detail. Also, the advances in in-silico and mathematical modelling would allow investigations into the mechanical strength, diffusion rates of growth factors, and structural and physical constraints.

Acknowledgements.

This work was supported by the National Institute of Health Award #U19AI142733 (I.T.O.).

Biographies



Irem Deniz Derman is a Ph.D. student at the Department of Engineering Science and Mechanics, Penn State University, USA. She received her M.Sc. from Istanbul Technical University, Istanbul, Turkey in 2018. Her research interests are 3D Bioprinting, biomaterials science and tissue engineering. Her current research is focused on developing lung tissue models.



Yogendra Pratap Singh is a Postdoctoral Scholar with Prof. Ozbolat at the Department of Engineering Science and Mechanics, Pennsylvania State University, USA. He received his Ph.D. from Indian Institute of Technology Guwahati, Assam, India in 2021. His research interests include 3D Bioprinting, biomaterials science, induced pluripotent stem cells, and disease models. His current research is focused on developing pancreatic devices for type 1 diabetes and periosteum regeneration.



Ibrahim Tarik Ozbolat is a Professor of Engineering Science and Mechanics, Biomedical Engineering and Neurosurgery, and a member of the Huck Institutes of the Life Sciences at Penn State University. Dr. Ozbolat's main area of research is in the field of 3D Bioprinting. He has been working on several aspects of bioprinting such as bioprinting processes, bioink materials, bioprinters and post-bioprinting tissue maturation for manufacturing of more than a dozen tissues and organs. Dr. Ozbolat is a leading scientist with over 150 publications, including two books in his domain. Due to his notable contributions to the field of bioprinting, he has received several prestigious international and national awards.

References

1. Quaderi SA & Hurst JR The unmet global burden of COPD. *Glob Health Epidemiol Genom* 3, e4 (2018). [PubMed: 29868229]
2. Skolasinski SD & Panoskaltis-Mortari A Lung tissue bioengineering for chronic obstructive pulmonary disease: overcoming the need for lung transplantation from human donors. *Expert Review of Respiratory Medicine* vol. 13 Preprint at 10.1080/17476348.2019.1624163 (2019).
3. Hoffman Matthew. Lung Transplant. <https://www.webmd.com/lung/lung-transplant-surgery> (2021).

4. Unilateral Lung Transplantation for Pulmonary Fibrosis. *New England Journal of Medicine* 314, 1140–1145 (1986). [PubMed: 3515192]
5. Taniguchi D et al. Scaffold-free trachea regeneration by tissue engineering with bio-3D printing. *Interact Cardiovasc Thorac Surg* 26, (2018).
6. van Riet S et al. In vitro modelling of alveolar repair at the air-liquid interface using alveolar epithelial cells derived from human induced pluripotent stem cells. *Sci Rep* 10, (2020).
7. Zamprogno P et al. Second-generation lung-on-a-chip with an array of stretchable alveoli made with a biological membrane. *Commun Biol* 4, (2021).
8. Wailoo MP & Emery JL Normal growth and development of the trachea. *Thorax* 37, (1982).
9. Gehr P Respiratory tract structure and function. *J Toxicol Environ Health* 13, (1984).
10. Horsfield K Diameters, generations, and orders of branches in the bronchial tree. *J Appl Physiol* 68, (1990).
11. Macklem PT The physiology of small airways. *American Journal of Respiratory and Critical Care Medicine* vol. 157 Preprint at 10.1164/ajrccm.157.5.rsaa-2 (1998).
12. Tomashefski JF, Cagle PT, Farver CF & Fraire AE Dail and Hammar's pulmonary pathology. *Dail and Hammar's Pulmonary Pathology* vol. 1 (2008).
13. Uriarte JJ, Uhl FE, Rolandsson Enes SE, Pouliot RA & Weiss DJ Lung bioengineering: advances and challenges in lung decellularization and recellularization. *Current Opinion in Organ Transplantation* vol. 23 Preprint at 10.1097/MOT.0000000000000584 (2018).
14. Calle EA, Leiby KL, Raredon MB & Niklason LE Lung regeneration: Steps toward clinical implementation and use. *Current Opinion in Anaesthesiology* vol. 30 Preprint at 10.1097/ACO.0000000000000425 (2017).
15. Tebyanian H et al. Lung tissue engineering: An update. *Journal of Cellular Physiology* vol. 234 Preprint at 10.1002/jcp.28558 (2019).
16. Tsuchiya T et al. Future prospects for tissue engineered lung transplantation. *Organogenesis* 10, (2014).
17. Baiguera S, Birchall MA & MacChiarini P Tissue-engineered tracheal transplantation. *Transplantation* vol. 89 Preprint at 10.1097/TP.0b013e3181cd4ad3 (2010).
18. Grillo HC Tracheal replacement: A critical review. *Annals of Thoracic Surgery* 73, (2002).
19. Belsey R Resection and reconstruction of the intrathoracic trachea. *British Journal of Surgery* 38, (1950).
20. Neville WE, Bolanowski PJP & Kotia GG Clinical experience with the silicone tracheal prosthesis. in *Journal of Thoracic and Cardiovascular Surgery* vol. 99 (1990).
21. Nelson RJ, Goldberg L, White RA, Shors E & Hirose FM Neovascularity of a tracheal prosthesis/tissue complex. *Journal of Thoracic and Cardiovascular Surgery* 86, (1983).
22. Rose KG, Sesterhenn K & Wustrow F TRACHEAL ALLOTRANSPLANTATION IN MAN. *The Lancet* vol. 313 Preprint at 10.1016/S0140-6736(79)90902-4 (1979).
23. Vacanti CA et al. Experimental tracheal replacement using tissue-engineered cartilage. *J Pediatr Surg* 29, (1994).
24. Macchiarini P et al. Clinical transplantation of a tissue-engineered airway. *The Lancet* 372, (2008).
25. Park JH et al. A novel tissue-engineered trachea with a mechanical behavior similar to native trachea. *Biomaterials* 62, (2015).
26. Park JH et al. Human turbinate mesenchymal stromal cell sheets with bellows graft for rapid tracheal epithelial regeneration. *Acta Biomater* 25, (2015).
27. Chang JW et al. Tissue-engineered tracheal reconstruction using three-dimensionally printed artificial tracheal graft: Preliminary report. *Artif Organs* 38, (2014).
28. Goldstein TA, Smith BD, Zeltsman D, Grande D & Smith LP Introducing a 3-dimensionally printed, tissue-engineered graft for airway reconstruction: A pilot study. in *Otolaryngology - Head and Neck Surgery (United States)* vol. 153 (2015).
29. Gao M et al. Tissue-engineered trachea from a 3D-printed scaffold enhances whole-segment tracheal repair. *Sci Rep* 7, (2017).
30. Townsend JM et al. Biodegradable electrospun patch containing cell adhesion or antimicrobial compounds for trachea repair in vivo. *Biomedical Materials (Bristol)* 15, (2020).

31. Gungor-Ozkerim PS, Inci I, Zhang YS, Khademhosseini A & Dokmeci MR Bioprinting for 3D bioprinting: An overview. *Biomaterials Science* vol. 6 Preprint at 10.1039/c7bm00765e (2018).
32. Unagolla JM & Jayasuriya AC Hydrogel-based 3D bioprinting: A comprehensive review on cell-laden hydrogels, bioink formulations, and future perspectives. *Applied Materials Today* vol. 18 Preprint at 10.1016/j.apmt.2019.100479 (2020).
33. Ovsianikov A, Khademhosseini A & Mironov V The Synergy of Scaffold-Based and Scaffold-Free Tissue Engineering Strategies. *Trends in Biotechnology* vol. 36 Preprint at 10.1016/j.tibtech.2018.01.005 (2018).
34. Banerjee D et al. Strategies for 3D bioprinting of spheroids: A comprehensive review. *Biomaterials* 291, 121881 (2022). [PubMed: 36335718]
35. Subia B, Kundu J & C. S Biomaterial Scaffold Fabrication Techniques for Potential Tissue Engineering Applications. in *Tissue Engineering* (2010). doi:10.5772/8581.
36. Safshekan F, Tafazzoli-Shadpour M, Abdouss M & Shadmehr MB Mechanical characterization and constitutive modeling of human trachea: Age and gender dependency. *Materials* 9, (2016).
37. Abdul Samat A, Abdul Hamid ZA, Jaafar M & Yahaya BH Mechanical properties and in vitro evaluation of thermoplastic polyurethane and polylactic acid blend for fabrication of 3d filaments for tracheal tissue engineering. *Polymers (Basel)* 13, (2021).
38. Hamilton NJI et al. Bioengineered airway epithelial grafts with mucociliary function based on collagen iv- And laminin-containing extracellular matrix scaffolds. *European Respiratory Journal* 55, (2020).
39. Kwon SK et al. Tracheal reconstruction with asymmetrically porous polycaprolactone/pluronic F127 membranes. *Head Neck* 36, (2014).
40. Grimmer JF et al. Tracheal reconstruction using tissue-engineered cartilage. *Archives of Otolaryngology - Head and Neck Surgery* 130, (2004).
41. Ghorbani F et al. In-vivo characterization of a 3D hybrid scaffold based on PCL/decellularized aorta for tracheal tissue engineering. *Materials Science and Engineering C* 81, (2017).
42. Siddiqi S Tissue Engineering of the Trachea: What is the Hold-up? *MOJ Cell Science & Report* 4, (2017).
43. Ke D et al. Bioprinted trachea constructs with patient-matched design, mechanical and biological properties. *Biofabrication* 12, (2020).
44. Bae SW et al. 3D bioprinted artificial trachea with epithelial cells and chondrogenic-differentiated bone marrow-derived mesenchymal stem cells. *Int J Mol Sci* 19, (2018).
45. Park JH et al. Experimental Tracheal Replacement Using 3-dimensional Bioprinted Artificial Trachea with Autologous Epithelial Cells and Chondrocytes. *Sci Rep* 9, (2019).
46. Machino R et al. Replacement of Rat Tracheas by Layered, Trachea-Like, Scaffold-Free Structures of Human Cells Using a Bio-3D Printing System. *Adv Healthc Mater* 8, (2019).
47. Almendros I et al. Lung extracellular matrix hydrogel for 3D bioprinting of lung mesenchymal stem cells. in *Mechanisms of lung injury and repair PA3859* (European Respiratory Society, 2019). doi:10.1183/13993003.congress-2019.PA3859.
48. Jungebluth P et al. Tracheal tissue engineering in rats. *Nature Protocols* vol. 9 Preprint at 10.1038/nprot.2014.149 (2014).
49. Athanasiou KA, Eswaramoorthy R, Hadidi P & Hu JC Self-organization and the self-assembling process in Tissue engineering. *Annual Review of Biomedical Engineering* vol. 15 Preprint at 10.1146/annurev-bioeng-071812-152423 (2013).
50. Liu X & Ma PX Polymeric scaffolds for bone tissue engineering. *Ann Biomed Eng* 32, (2004).
51. Meredith JC et al. Combinatorial characterization of cell interactions with polymer surfaces. *J Biomed Mater Res A* 66, (2003).
52. Barbero A, Grogan SP, Mainil-Varlet P & Martin I Expansion on specific substrates regulates the phenotype and differentiation capacity of human articular chondrocytes. *J Cell Biochem* 98, (2006).
53. Bryant SJ, Anseth KS, Lee DA & Bader DL Crosslinking density influences the morphology of chondrocytes photoencapsulated in PEG hydrogels during the application of compressive strain. *Journal of Orthopaedic Research* 22, (2004).

54. Anderson JM Biological responses to materials. *Annual Review of Materials Science* 31, (2001).
55. Valdoz JC et al. The ECM: To scaffold, or not to scaffold, that is the question. *International Journal of Molecular Sciences* vol. 22 Preprint at 10.3390/ijms222312690 (2021).
56. Taniguchi D et al. Human lung microvascular endothelial cells as potential alternatives to human umbilical vein endothelial cells in bio-3D-printed trachea-like structures. *Tissue Cell* 63, (2020).
57. Wendt D, Marsano A, Jakob M, Heberer M & Martin I Oscillating perfusion of cell suspensions through three-dimensional scaffolds enhances cell seeding efficiency and uniformity. *Biotechnol Bioeng* 84, (2003).
58. Wendt D, Riboldi SA, Cioffi M & Martin I Bioreactors in tissue engineering: Scientific challenges and clinical perspectives. *Advances in Biochemical Engineering/Biotechnology* vol. 112 Preprint at 10.1007/978-3-540-69357-4_1 (2009).
59. Elliott MJ et al. Stem-cell-based, tissue engineered tracheal replacement in a child: A 2-year follow-up study. *The Lancet* 380, (2012).
60. Lin CH, Hsu S, hui, Huang CE, Cheng WT & Su JM A scaffold-bioreactor system for a tissue-engineered trachea. *Biomaterials* 30, (2009).
61. Zhou H et al. Bioengineering Human Lung Grafts on Porcine Matrix. *Ann Surg* 267, (2018).
62. Ghaedi M et al. Alveolar epithelial differentiation of human induced pluripotent stem cells in a rotating bioreactor. *Biomaterials* 35, (2014).
63. Si L et al. A human-airway-on-a-chip for the rapid identification of candidate antiviral therapeutics and prophylactics. *Nat Biomed Eng* 5, (2021).
64. Zampetaki A, Kirton JP & Xu Q Vascular repair by endothelial progenitor cells. *Cardiovascular Research* vol. 78 Preprint at 10.1093/cvr/cvn081 (2008).
65. Laschke MW & Menger MD Prevascularization in tissue engineering: Current concepts and future directions. *Biotechnology Advances* vol. 34 Preprint at 10.1016/j.biotechadv.2015.12.004 (2016).
66. Mertsching H, Walles T, Hofmann M, Schanz J & Knapp WH Engineering of a vascularized scaffold for artificial tissue and organ generation. *Biomaterials* 26, (2005).
67. Walles T et al. Experimental generation of a tissue-engineered functional and vascularized trachea. *Journal of Thoracic and Cardiovascular Surgery* 128, (2004).
68. Kim J et al. Replacement of a tracheal defect with a tissue-engineered prosthesis: Early results from animal experiments. *Journal of Thoracic and Cardiovascular Surgery* 128, (2004).
69. Luo X et al. Long-term functional reconstruction of segmental tracheal defect by pedicled tissue-engineered trachea in rabbits. *Biomaterials* 34, (2013).
70. Haykal S et al. Double-chamber rotating bioreactor for dynamic perfusion cell seeding of large-segment tracheal allografts: Comparison to conventional static methods. *Tissue Eng Part C Methods* 20, (2014).
71. Ruszymah BHI, Chua K, Latif MA, Nor Hussein F & bin Saim A Formation of in vivo tissue engineered human hyaline cartilage in the shape of a trachea with internal support. *Int J Pediatr Otorhinolaryngol* 69, (2005).
72. Kajbafzadeh AM et al. In-vivo trachea regeneration: fabrication of a tissue-engineered trachea in nude mice using the body as a natural bioreactor. *Surg Today* 45, (2015).
73. Pearl AW, Gannon PJ & Urken ML Anatomy and vascular perfusion territories of the superior thyroid artery in *Macaca mulatta*. *Laryngoscope* 108, (1998).
74. Ahn CB et al. Development of a flexible 3D printed scaffold with a cell-adhesive surface for artificial trachea. *Biomedical Materials (Bristol)* 14, (2019).
75. Lei C, Mei S, Zhou C & Xia C Decellularized tracheal scaffolds in tracheal reconstruction: An evaluation of different techniques. *Journal of Applied Biomaterials and Functional Materials* vol. 19 Preprint at 10.1177/22808000211064948 (2021).
76. Matsubara Y et al. Prosthetic reconstruction of the trachea and carina. *Nippon Geka Gakkai zasshi* 88, (1987).
77. Toomes H, Mickisch G & Vogt-Moykopf I Experiences with prosthetic reconstruction of the trachea and bifurcation. *Thorax* 40, (1985).
78. Lee JY, Park JH & Cho DW Comparison of tracheal reconstruction with allograft, fresh xenograft and artificial trachea scaffold in a rabbit model. *Journal of Artificial Organs* 21, (2018).

79. Pepper V et al. Factors Influencing Poor Outcomes in Synthetic Tissue-Engineered Tracheal Replacement. *Otolaryngology - Head and Neck Surgery (United States)* 161, (2019).
80. Wurtz A et al. Surgical technique and results of tracheal and carinal replacement with aortic allografts for salivary gland-type carcinoma. *Journal of Thoracic and Cardiovascular Surgery* 140, (2010).
81. Moghissi K Tracheal reconstruction with a prosthesis of Marlex mesh and pericardium. *Journal of Thoracic and Cardiovascular Surgery* 69, (1975).
82. Levitzky MG Function and structure of the respiratory system. *Lange physiology series pulmonary physiology* (2007).
83. Petersen TH et al. Tissue-engineered lungs for in vivo implantation. *Science* (1979) 329, (2010).
84. Ott HC et al. Regeneration and orthotopic transplantation of a bioartificial lung. *Nat Med* 16, (2010).
85. Leiby KL & Niklason LE Lung Tissue Engineering: Toward a More Deliberate Approach. *ACS Biomater Sci Eng* (2021) doi:10.1021/acsbiomaterials.1c01392.
86. Ohata K & Ott HC Human-scale lung regeneration based on decellularized matrix scaffolds as a biologic platform. *Surgery Today* vol. 50 Preprint at 10.1007/s00595-020-02000-y (2020).
87. Gilpin SE et al. Regenerative potential of human airway stem cells in lung epithelial engineering. *Biomaterials* 108, (2016).
88. Ghaedi M et al. Bioengineered lungs generated from human iPSCs-derived epithelial cells on native extracellular matrix. *J Tissue Eng Regen Med* 12, (2018).
89. Ghaedi M et al. Human iPSC cell-derived alveolar epithelium repopulates lung extracellular matrix. *Journal of Clinical Investigation* 123, (2013).
90. Akinola I et al. Engineering Functional Vasculature in Decellularized Lungs Depends on Comprehensive Endothelial Cell Tropism. *Front Bioeng Biotechnol* 9, (2021).
91. Scarritt ME et al. Re-endothelialization of rat lung scaffolds through passive, gravity-driven seeding of segment-specific pulmonary endothelial cells. *J Tissue Eng Regen Med* 12, (2018).
92. Ren X et al. Engineering pulmonary vasculature in decellularized rat and human lungs. *Nat Biotechnol* 33, (2015).
93. Badyalak SF, Taylor D & Uygun K Whole-organ tissue engineering: Decellularization and recellularization of three-dimensional matrix scaffolds. *Annu Rev Biomed Eng* 13, (2011).
94. Wallis JM et al. Comparative assessment of detergent-based protocols for mouse lung decellularization and re-cellularization. *Tissue Eng Part C Methods* 18, (2012).
95. Zhou Y et al. Extracellular matrix in lung development, homeostasis and disease. *Matrix Biology* vol. 73 Preprint at 10.1016/j.matbio.2018.03.005 (2018).
96. Park JY et al. Development of a functional airway-on-a-chip by 3D cell printing. *Biofabrication* 11, (2019).
97. Guo K et al. Collagen-Based Thiol-Norbornene Photoclick Bio-Ink with Excellent Bioactivity and Printability. *ACS Appl Mater Interfaces* 13, (2021).
98. Tijore A et al. Contact guidance for cardiac tissue engineering using 3D bioprinted gelatin patterned hydrogel. *Biofabrication* 10, (2018).
99. Hospodiuk M, Dey M, Sosnoski D & Ozbolat IT The bioink: A comprehensive review on bioprintable materials. *Biotechnology Advances* vol. 35 Preprint at 10.1016/j.biotechadv.2016.12.006 (2017).
100. Kabirian F & Mozafari M Decellularized ECM-derived bioinks: Prospects for the future. *Methods* vol. 171 Preprint at 10.1016/j.ymeth.2019.04.019 (2020).
101. Barreiro Carpio M et al. 3D Bioprinting Strategies, Challenges, and Opportunities to Model the Lung Tissue Microenvironment and Its Function. *Frontiers in Bioengineering and Biotechnology* vol. 9 Preprint at 10.3389/fbioe.2021.773511 (2021).
102. Grigoryan B et al. Multivascular networks and functional intravascular topologies within biocompatible hydrogels. *Science* (1979) 364, (2019).
103. Horvath L et al. Engineering an in vitro air-blood barrier by 3D bioprinting. *Sci Rep* 5, (2015).
104. Ng WL et al. Fabrication and Characterization of 3D Bioprinted Triple-layered Human Alveolar Lung Models. *Int J Bioprint* 7, (2021).

105. Kang D et al. All-Inkjet-Printed 3D Alveolar Barrier Model with Physiologically Relevant Microarchitecture. *Advanced Science* 8, (2021).
106. Kabir A et al. 3D Bioprinting for fabrication of tissue models of COVID-19 infection. *Essays in Biochemistry* vol. 65 Preprint at 10.1042/EBC20200129 (2021).
107. Ayan B et al. Aspiration-assisted bioprinting for precise positioning of biologics. *Sci Adv* 6, (2020).
108. Rodrigues AL et al. Dissolvable Microcarriers Allow Scalable Expansion And Harvesting Of Human Induced Pluripotent Stem Cells Under Xeno-Free Conditions. *Biotechnol J* 14, (2019).
109. Panoskaltis-Mortari A Bioreactor Development for Lung Tissue Engineering. *Curr Transplant Rep* 2, (2015).
110. Petersen TH, Calle EA, Colehour MB & Niklason LE Bioreactor for the long-term culture of lung tissue. *Cell Transplant* 20, (2011).
111. Arold SP, Wong JY & Suki B Design of a new stretching apparatus and the effects of cyclic strain and substratum on mouse lung epithelial-12 cells. *Ann Biomed Eng* 35, (2007).
112. Bonvillain RW et al. Nonhuman primate lung decellularization and recellularization using a specialized large-organ bioreactor. *J Vis Exp* (2013) doi:10.3791/50825.
113. Huang D et al. Reversed-engineered human alveolar lung-on-a-chip model. *Proc Natl Acad Sci U S A* 118, (2021).
114. Zhang B & Radisic M Organ-on-A-chip devices advance to market. *Lab on a Chip* vol. 17 Preprint at 10.1039/c6lc01554a (2017).
115. Huh D et al. Reconstituting organ-level lung functions on a chip. *Science* (1979) 328, (2010).
116. Stucki AO et al. A lung-on-a-chip array with an integrated bio-inspired respiration mechanism. *Lab Chip* 15, (2015).
117. Tajeddin A & Mustafaoglu N Design and fabrication of organ-on-chips: Promises and challenges. *Micromachines (Basel)* 12, (2021).
118. Huh D, Hamilton GA & Ingber DE From 3D cell culture to organs-on-chips. *Trends in Cell Biology* vol. 21 Preprint at 10.1016/j.tcb.2011.09.005 (2011).
119. Bein A et al. Microfluidic Organ-on-a-Chip Models of Human Intestine. *CMGH* vol. 5 Preprint at 10.1016/j.jcmgh.2017.12.010 (2018).
120. Lee JN, Park C & Whitesides GM Solvent Compatibility of Poly(dimethylsiloxane)-Based Microfluidic Devices. *Anal Chem* 75, (2003).
121. Abate AR, Lee D, Do T, Holtze C & Weitz DA Glass coating for PDMS microfluidic channels by sol-gel methods. *Lab Chip* 8, (2008).
122. Roman GT & Culbertson CT Surface engineering of poly(dimethylsiloxane) microfluidic devices using transition metal sol-gel chemistry. *Langmuir* 22, (2006).
123. Regehr KJ et al. Biological implications of polydimethylsiloxane-based microfluidic cell culture. *Lab on a Chip* vol. 9 Preprint at 10.1039/b903043c (2009).
124. Berthier E, Young EWK & Beebe D Engineers are from PDMS-land, biologists are from polystyrenia. *Lab on a Chip* vol. 12 Preprint at 10.1039/c2lc20982a (2012).
125. Dunphy SE, Bratt JAJ, Akram KM, Forsyth NR & el Haj AJ Hydrogels for lung tissue engineering: Biomechanical properties of thin collagen-elastin constructs. *J Mech Behav Biomed Mater* 38, (2014).
126. Chen S, Einspanier R & Schoen J Transepithelial electrical resistance (TEER): a functional parameter to monitor the quality of oviduct epithelial cells cultured on filter supports. *Histochem Cell Biol* 144, (2015).
127. Harrington H et al. Immunocompetent 3D model of human upper airway for disease modeling and in vitro drug evaluation. *Mol Pharm* 11, (2014).
128. Srinivasan B et al. TEER Measurement Techniques for In Vitro Barrier Model Systems. *Journal of Laboratory Automation* vol. 20 Preprint at 10.1177/2211068214561025 (2015).
129. Barkauskas CE et al. Type 2 alveolar cells are stem cells in adult lung. *Journal of Clinical Investigation* 123, (2013).
130. Barkauskas CE et al. Lung organoids: Current uses and future promise. *Development (Cambridge)* vol. 144 Preprint at 10.1242/dev.140103 (2017).

131. Chen YW et al. A three-dimensional model of human lung development and disease from pluripotent stem cells. *Nat Cell Biol* 19, (2017).
132. Jacob A et al. Differentiation of Human Pluripotent Stem Cells into Functional Lung Alveolar Epithelial Cells. *Cell Stem Cell* 21, (2017).
133. Sachs N et al. Long-term expanding human airway organoids for disease modeling. *EMBO J* 38, (2019).
134. Tindle C et al. Adult stem cell-derived complete lung organoid models emulate lung disease in COVID-19. *Elife* 10, (2021).
135. Georgios Stroulios TBGMDKADAESLJHWCDPKCWAS & Apical-out SS airway organoids as a platform for studying viral infections and screening for antiviral drugs. *Scientific Reports* volume (2022).
136. Li Y, Tang P, Cai S, Peng J & Hua G Organoid based personalized medicine: from bench to bedside. *Cell Regeneration* vol. 9 Preprint at 10.1186/s13619-020-00059-z (2020).
137. Huh D et al. Acoustically detectable cellular-level lung injury induced by fluid mechanical stresses in microfluidic airway systems. *Proc Natl Acad Sci U S A* 104, (2007).
138. Ferkol T & Schraufnagel D The global burden of respiratory disease. *Annals of the American Thoracic Society* vol. 11 Preprint at 10.1513/AnnalsATS.201311-405PS (2014).
139. Nichols JE & Cortiella J Engineering of a complex organ: Progress toward development of a tissue-engineered lung. in *Proceedings of the American Thoracic Society* vol. 5 (2008).
140. Singh YP, Moses JC, Bandyopadhyay A & Mandal BB 3D Bioprinted Silk-Based In Vitro Osteochondral Model for Osteoarthritis Therapeutics. *Adv Healthc Mater* 2200209 (2022) doi:10.1002/adhm.202200209.
141. Singh YP, Moses JC, Bhardwaj N & Mandal BB Overcoming the Dependence on Animal Models for Osteoarthritis Therapeutics – The Promises and Prospects of In Vitro Models. *Advanced Healthcare Materials* vol. 10 Preprint at 10.1002/adhm.202100961 (2021).
142. Longmire TA et al. Efficient derivation of purified lung and thyroid progenitors from embryonic stem cells. *Cell Stem Cell* 10, (2012).
143. Mou H et al. Generation of multipotent lung and airway progenitors from mouse ESCs and patient-specific cystic fibrosis iPSCs. *Cell Stem Cell* 10, (2012).
144. Crane AM et al. Targeted correction and restored function of the CFTR gene in cystic fibrosis induced pluripotent stem cells. *Stem Cell Reports* 4, (2015).
145. Gjorevski N et al. Designer matrices for intestinal stem cell and organoid culture. *Nature* 539, (2016).
146. Schneeberger K et al. Converging biofabrication and organoid technologies: The next frontier in hepatic and intestinal tissue engineering? *Biofabrication* vol. 9 Preprint at 10.1088/1758-5090/aa6121 (2017).
147. Huh D et al. Reconstituting organ-level lung functions on a chip. *Science* (1979) 328, (2010).
148. Sellgren KL, Butala EJ, Gilmour BP, Randell SH & Grego S A biomimetic multicellular model of the airways using primary human cells. *Lab Chip* 14, (2014).
149. Benam KH et al. Small airway-on-a-chip enables analysis of human lung inflammation and drug responses in vitro. *Nat Methods* 13, (2016).
150. Nesmith AP, Agarwal A, McCain ML & Parker KK Human airway musculature on a chip: An in vitro model of allergic asthmatic bronchoconstriction and bronchodilation. *Lab Chip* 14, (2014).
151. Hurley J v. Current views on the mechanisms of pulmonary oedema. *J Pathol* 125, (1978).
152. Jain A et al. Primary Human Lung Alveolus-on-a-chip Model of Intravascular Thrombosis for Assessment of Therapeutics. *Clin Pharmacol Ther* 103, (2018).
153. Tavana H et al. Dynamics of liquid plugs of buffer and surfactant solutions in a micro-engineered pulmonary airway model. *Langmuir* 26, (2010).
154. Hassell BA et al. Human Organ Chip Models Recapitulate Orthotopic Lung Cancer Growth, Therapeutic Responses, and Tumor Dormancy In Vitro. *Cell Rep* 21, (2017).
155. Felder M, Stucki AO, Stucki JD, Geiser T & Guenat OT The potential of microfluidic lung epithelial wounding: Towards in vivo-like alveolar microinjuries. *Integrative Biology (United Kingdom)* 6, (2014).

156. Tschumperlin DJ & Drazen JM Mechanical stimuli to airway remodeling. *Am J Respir Crit Care Med* 164, (2001).
157. Miller C, George S & Niklason L Developing a tissue-engineered model of the human bronchiole. *J Tissue Eng Regen Med* 4, (2010).4
158. Langhans SA Three-dimensional in vitro cell culture models in drug discovery and drug repositioning. *Frontiers in Pharmacology* vol. 9 Preprint at 10.3389/fphar.2018.00006 (2018).
159. Herrera J, Henke CA & Bitterman PB Extracellular matrix as a driver of progressive fibrosis. *Journal of Clinical Investigation* vol. 128 Preprint at 10.1172/JCI93557 (2018).
160. LaValley DJ & Reinhart-King CA Matrix stiffening in the formation of blood vessels. *Advances in Regenerative Biology* 1, (2014).
161. Barkal LJ et al. Microbial volatile communication in human organotypic lung models. *Nat Commun* 8, (2017).
162. Morrison RJ et al. Mitigation of tracheobronchomalacia with 3D-printed personalized medical devices in pediatric patients. *Sci Transl Med* 7, (2015).
163. Tam MD, Laycock SD, Jayne D, Babar J & Noble B 3-D printouts of the tracheobronchial tree generated from CT images as an aid to management in a case of tracheobronchial chondromalacia caused by relapsing polychondritis. *J Radiol Case Rep* 7, (2013).
164. Kurenov SN, Ionita C, Sammons D & Demmy TL Three-dimensional printing to facilitate anatomic study, device development, simulation, and planning in thoracic surgery. *Journal of Thoracic and Cardiovascular Surgery* 149, (2015).
165. Zopf DA, Flanagan CL, Wheeler M, Hollister SJ & Green GE Treatment of severe porcine tracheomalacia with a 3-dimensionally printed, bioresorbable, external airway splint. *JAMA Otolaryngol Head Neck Surg* 140, (2014).
166. Huang L et al. Tracheal suspension by using 3-dimensional printed personalized scaffold in a patient with tracheomalacia. *J Thorac Dis* 8, (2016).
167. Hollister SJ et al. Design Control for Clinical Translation of 3D Printed Modular Scaffolds. *Ann Biomed Eng* 43, (2015).
168. Les AS et al. 3D-printed, externally-implanted, bioresorbable airway splints for severe tracheobronchomalacia. *Laryngoscope* 129, (2019).
169. Huh D et al. A human disease model of drug toxicity-induced pulmonary edema in a lung-on-a-chip microdevice. *Sci Transl Med* 4, (2012).
170. Martonen T, Fleming J, Schroeter J, Conway J & Hwang D In silico modeling of asthma. in *Advanced Drug Delivery Reviews* vol. 55 (2003).
171. Nowak N, Kakade PP & Annappagada A v. Computational fluid dynamics simulation of airflow and aerosol deposition in human lungs. *Ann Biomed Eng* 31, (2003).
172. Annappagada A & Mishchiy N In silico modeling of aerosol deposition in lungs. *Drug Discovery Today: Disease Models* vol. 4 Preprint at 10.1016/j.ddmod.2007.11.004 (2007).
173. Ma B et al. CFD simulation and experimental validation of fluid flow and particle transport in a model of alveolated airways. *J Aerosol Sci* 40, (2009).
174. Hansen JE, Ampaya EP, Bryant GH & Navin JJ Branching pattern of airways and air spaces of a single human terminal bronchiole. *J Appl Physiol* 38, (1975).
175. Ma B & Darquenne C Aerosol deposition characteristics in distal acinar airways under cyclic breathing conditions. *J Appl Physiol* 110, (2011).
176. Koshiyama K & Wada S Mathematical model of a heterogeneous pulmonary acinus structure. *Comput Biol Med* 62, (2015).
177. Koullapis PG, Hofemeier P, Sznitman J & Kassinos SC An efficient computational fluid-particle dynamics method to predict deposition in a simplified approximation of the deep lung. *European Journal of Pharmaceutical Sciences* 113, (2018).
178. Poorbahrami K, Vignon-Clementel IE, Shadden SC & Oakes JM A whole lung in silico model to estimate age dependent particle dosimetry. *Sci Rep* 11, (2021).
179. Singh YP, Moses JC, Bhardwaj N & Mandal BB Overcoming the Dependence on Animal Models for Osteoarthritis Therapeutics – The Promises and Prospects of In Vitro Models. *Advanced Healthcare Materials* vol. 10 Preprint at 10.1002/adhm.202100961 (2021).

180. Dabak G & enbaklavaci Ö History of lung transplantation. *Turk Toraks Dergisi* vol. 17 Preprint at 10.5578/ttj.17.2.014 (2016).
181. Reitz BA et al. Heart-lung transplantation - successful therapy for patients with pulmonary vascular disease. *N Engl J Med* 306, (1982).
182. Mount Sinai Surgeons Perform First Human Tracheal Transplant Surgery. (2021).
183. Delaere P, Vranckx J, Verleden G, de Leyn P & van Raemdonck D Tracheal Allograft Transplantation after Withdrawal of Immunosuppressive Therapy. *New England Journal of Medicine* 362, (2010).
184. Ingenito EP et al. Bronchoscopic lung volume reduction using tissue engineering principles. *Am J Respir Crit Care Med* 167, (2003).
185. Hamilton NJ et al. Tissue-Engineered Tracheal Replacement in a Child: A 4-Year Follow-Up Study. *American Journal of Transplantation* 15, (2015).
186. Elliott MJ et al. Tracheal replacement therapy with a stem cell-seeded graft: Lessons from compassionate use application of a GMP-compliant tissue-engineered medicine. *Stem Cells Transl Med* 6, (2017).
187. Kim IG et al. Transplantation of a 3D-printed tracheal graft combined with iPS cell-derived MSCs and chondrocytes. *Sci Rep* 10, (2020).
188. Collum SD et al. Pulmonary Hypertension Associated with Idiopathic Pulmonary Fibrosis: Current and Future Perspectives. *Canadian Respiratory Journal* vol. 2017 Preprint at 10.1155/2017/1430350 (2017).
189. Datta A, Scotton CJ & Chambers RC Novel therapeutic approaches for pulmonary fibrosis. *British Journal of Pharmacology* vol. 163 Preprint at 10.1111/j.1476-5381.2011.01247.x (2011).
190. Calvello M, Flore MC & Richeldi L Novel drug targets in idiopathic pulmonary fibrosis. *Expert Opinion on Orphan Drugs* vol. 7 Preprint at 10.1080/21678707.2019.1590196 (2019).
191. Barkauskas CE & Noble PW Cellular Mechanisms of Tissue Fibrosis. 7. New insights into the cellular mechanisms of pulmonary fibrosis. *Am J Physiol Cell Physiol* 306, (2014).
192. Sava P et al. Human pericytes adopt myofibroblast properties in the microenvironment of the IPF lung. *JCI Insight* 2, (2017).
193. Skronska-Wasek W et al. Reduced frizzled receptor 4 expression prevents WNT/b-catenin-driven alveolar lung repair in chronic obstructive pulmonary disease. *Am J Respir Crit Care Med* 196, (2017).
194. Ravnicek DJ et al. Transplantation of Bioprinted Tissues and Organs. *Ann Surg* 266, (2017).
195. Low LA, Mummery C, Berridge BR, Austin CP & Tagle DA Organs-on-chips: into the next decade. *Nature Reviews Drug Discovery* vol. 20 Preprint at 10.1038/s41573-020-0079-3 (2021).
196. Pound P Are animal models needed to discover, develop and test pharmaceutical drugs for humans in the 21st century? *Animals* vol. 10 Preprint at 10.3390/ani10122455 (2020).
197. Mallea JM et al. Remote ex vivo lung perfusion at a centralized evaluation facility. *The Journal of Heart and Lung Transplantation* (2022) doi:10.1016/j.healun.2022.09.006.
198. Zhao X et al. Ventricular flow analysis and its association with exertional capacity in repaired tetralogy of Fallot: 4D flow cardiovascular magnetic resonance study. *Journal of Cardiovascular Magnetic Resonance* 24, (2022).
199. Leng S et al. Cardiovascular magnetic resonance-assessed fast global longitudinal strain parameters add diagnostic and prognostic insights in right ventricular volume and pressure loading disease conditions. *Journal of Cardiovascular Magnetic Resonance* 23, (2021).
200. Hallberg CJ et al. Treatment of asthma exacerbations with the human-powered nebuliser: A randomised parallel-group clinical trial. *NPJ Prim Care Respir Med* 24, (2014).
201. Corcoran TE et al. Absorptive clearance of DTPA as an aerosol-based biomarker in the cystic fibrosis airway. *European Respiratory Journal* 35, (2010).
202. Lin M et al. Clinical efficacy of percutaneous cryoablation combined with allogeneic NK cell immunotherapy for advanced non-small cell lung cancer. *Immunol Res* 65, (2017).
203. Ramalingam SS et al. A phase 1/2 study of ADXS-503 alone and in combination with pembrolizumab in subjects with metastatic squamous or non-squamous non-small cell lung cancer (NSCLC). *Journal of Clinical Oncology* 38, e21682–e21682 (2020).

204. Hamilton SJ & Mueller JL Direct EIT reconstructions of complex admittivities on a chest-shaped Domain in 2-D. *IEEE Trans Med Imaging* 32, (2013).
205. Aliverti A et al. Human respiratory muscle actions and control during exercise. *J Appl Physiol* 83, (1997).

Author Manuscript

Author Manuscript

Author Manuscript

Author Manuscript

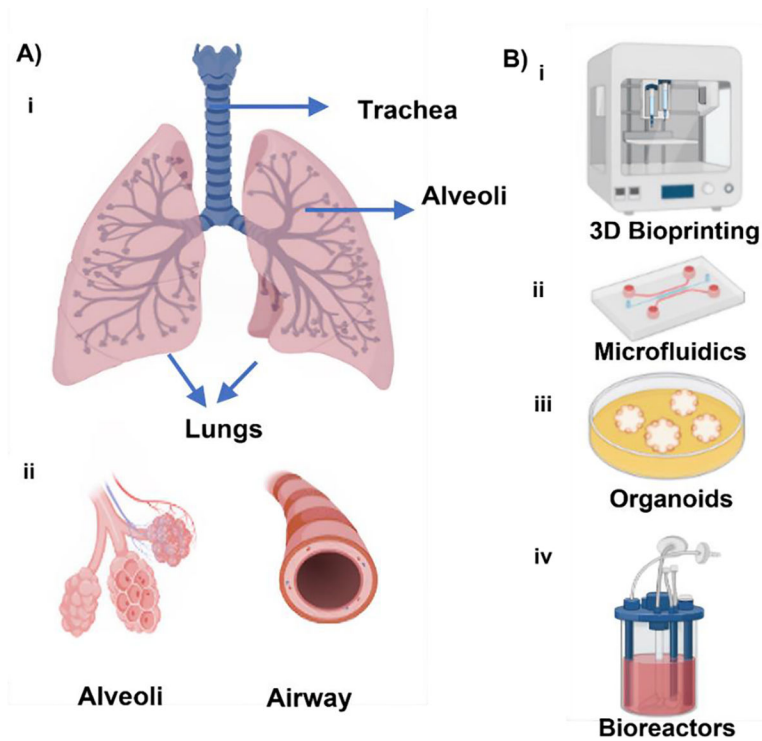


Figure 1: A) Anatomy of the respiratory system and B) the primary bioengineering approaches, including i) 3D (bio)printing, ii) microfluidics, iii) organoids, and iv) bioreactors for reconstituting lung and its components (created using [BioRender.com](https://www.biorender.com/)).

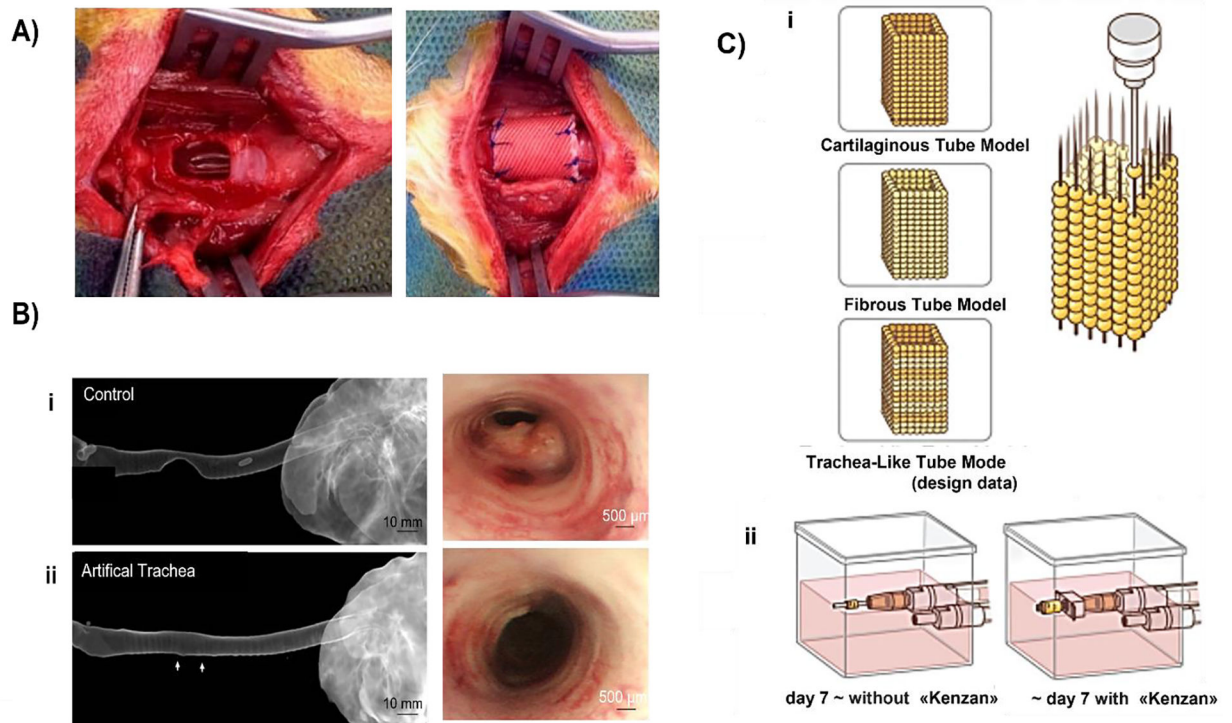


Figure 2:

A) Application of an artificial trachea made via 3D bioprinting (adapted and reproduced with permission from⁴⁴). B) Photographs from a bronchoscopy and computed tomography: i) control group versus ii) the experimental group (adapted and reproduced with permission from⁴⁵). C) A schematic drawing demonstrating the creation of tubes. i) Three different tube types were fabricated using the “Kenzan” method and ii) matured under an appropriate medium flow (adapted and reproduced with permission from⁴⁶).

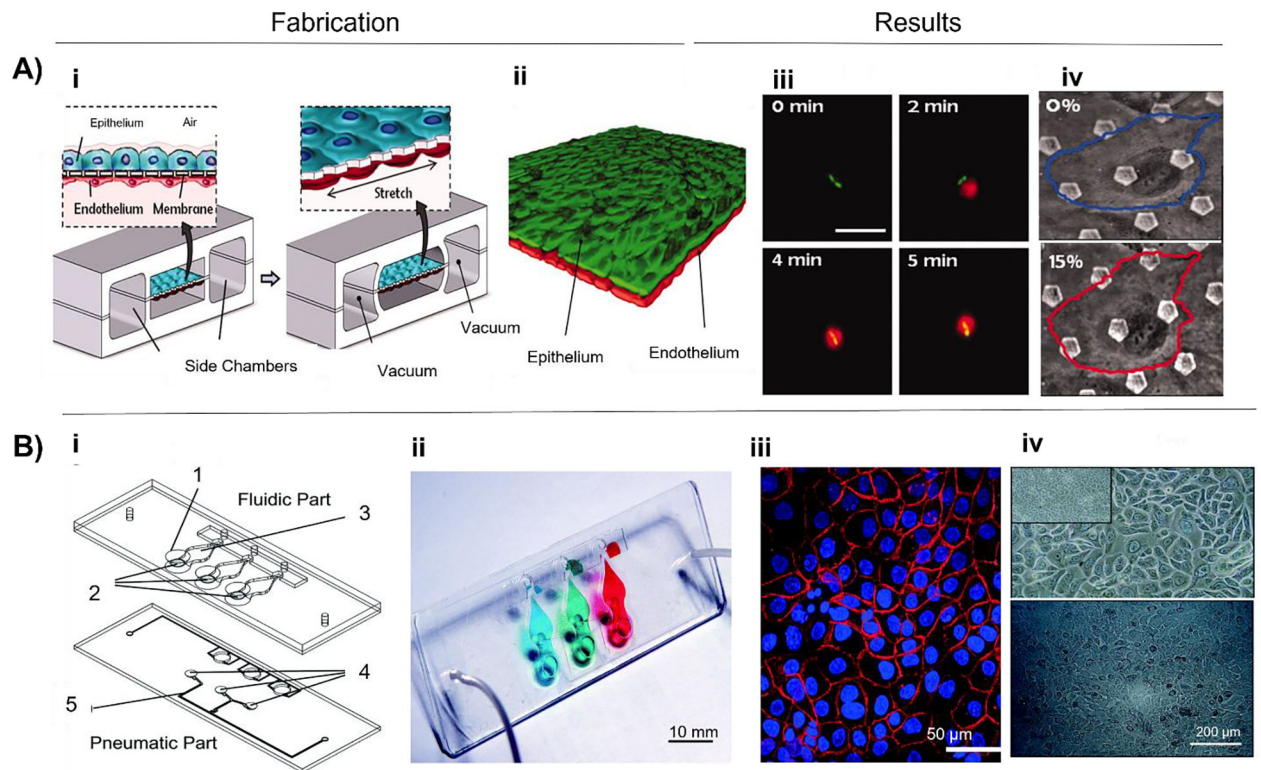


Figure 3: Fabrication of lung-on-a-chip models. A) i) The segmented PDMS microchannels in a microfabricated device was separated by an alveolar-capillary barrier using a thin, porous, flexible PDMS membrane coated with ECM. By applying suction to side chambers and mechanically stretching the PDMS membrane that makes up the alveolar-capillary barrier, the device simulated the physiological breathing motions. ii) A monolayer of the microvascular endothelium and a single layer of the alveolar epithelium were intimately apposed at the tissue-tissue interface created by long-term microfluidic coculture. iii) Fluorescence time-lapse images depict a neutrophil (red) moving from the vascular microchannel to the alveolar compartment phagocytosing two GFP-expressing *E. coli* bacteria on the epithelial surface. iv) Cells were under strain from membrane stretching, which caused them to warp in the direction of the applied force (adapted and reproduced with permission from¹¹⁵). B) i) Fluidic and pneumatic components measured by 25×75 mm made up the lung-on-a-chip. Three alveolar cell culture wells (1) and thin, porous, and flexible membranes (2), on top of which the basolateral chambers were situated, make up the fluidic component (3). The pneumatic component integrated micro-diaphragms (4) that were coupled to pneumatic microchannels. ii) An image showing the basolateral chambers of the lung-on-a-chip with food-dye color solutions. iii) Lung epithelial cells stained for adherents junction E-cadherin (red) and cell nuclei (blue) iv) Epithelial cell adhesion molecule (*EpCAM*)⁺ HPAECs expanded in culture are shown in a representative phase contrast image (upper) and a phase-contrast image (lower) of an alveolar membrane-grown confluent monolayer of *EpCAM*⁺ HPAECs (adapted and reproduced with permission from¹¹⁶).

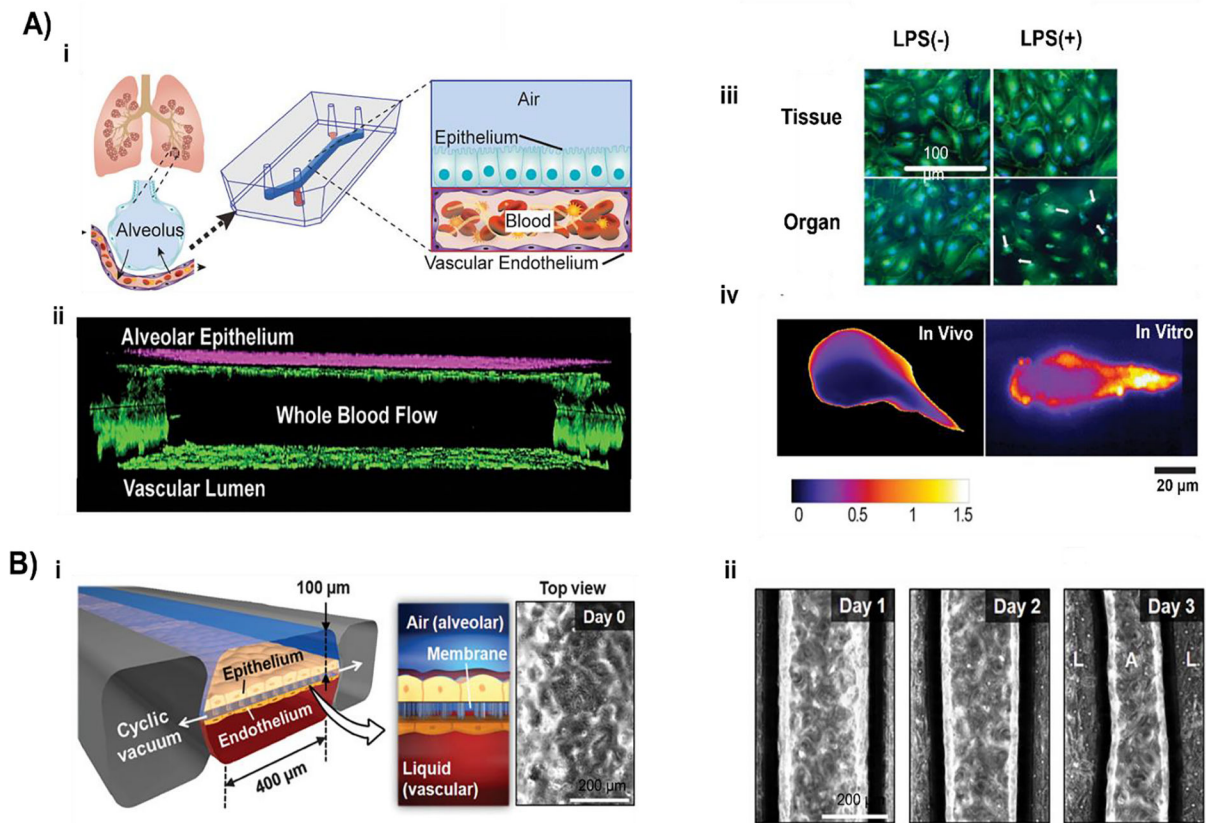


Figure 4.

In vitro disease models: A) i) A schematic of the human lung that illustrates how, during hemostasis or pulmonary dysfunction, the alveoli interact with the nearby blood arteries. Illustration of the microdevice that replicates the microarchitecture of the alveolar-capillary interface by separating two compartments made of PDMS with a thin, porous membrane. The bottom chamber was lined up with human endothelial cells, providing a lumen, while the top compartment was cultivated with human primary alveolar epithelial cells. Fluorescence microscopy was used to monitor thrombus development as the whole blood was perfused through the bottom chamber. ii) After 12 days of coculture, junctional structures were visible in the side view of confocal micrographs of the bottom chamber. iii) Representative confocal images demonstrating that when lipopolysaccharide was administered to the chip containing the epithelium and endothelium in an organ, but not when applied to the endothelium alone, VE cadherin-labeled endothelial cell-cell adhesions (green) opened and contracted. iv) The color-coded image below displayed the coefficient of variation within laser-induced thrombus in vivo and TNF (tumor necrosis factor)-induced thrombus on vascular lumen in vitro (adapted and reproduced with permission from¹⁵²). B) i) A lung-on-a-chip that mimics the microarchitecture of the lung and the breathing-induced cyclic mechanical distortion of the alveolar-capillary interface was used to replicate the IL-2-induced pulmonary edema. Alveolar channels were located at the top, and vascular channels were located at the bottom. ii) Liquid in the lower microvascular channel leaked into the alveolar chamber because of endothelial exposure to interleukin-2 (Days 1 to 3) (adapted and reproduced with permission from¹⁶⁹).

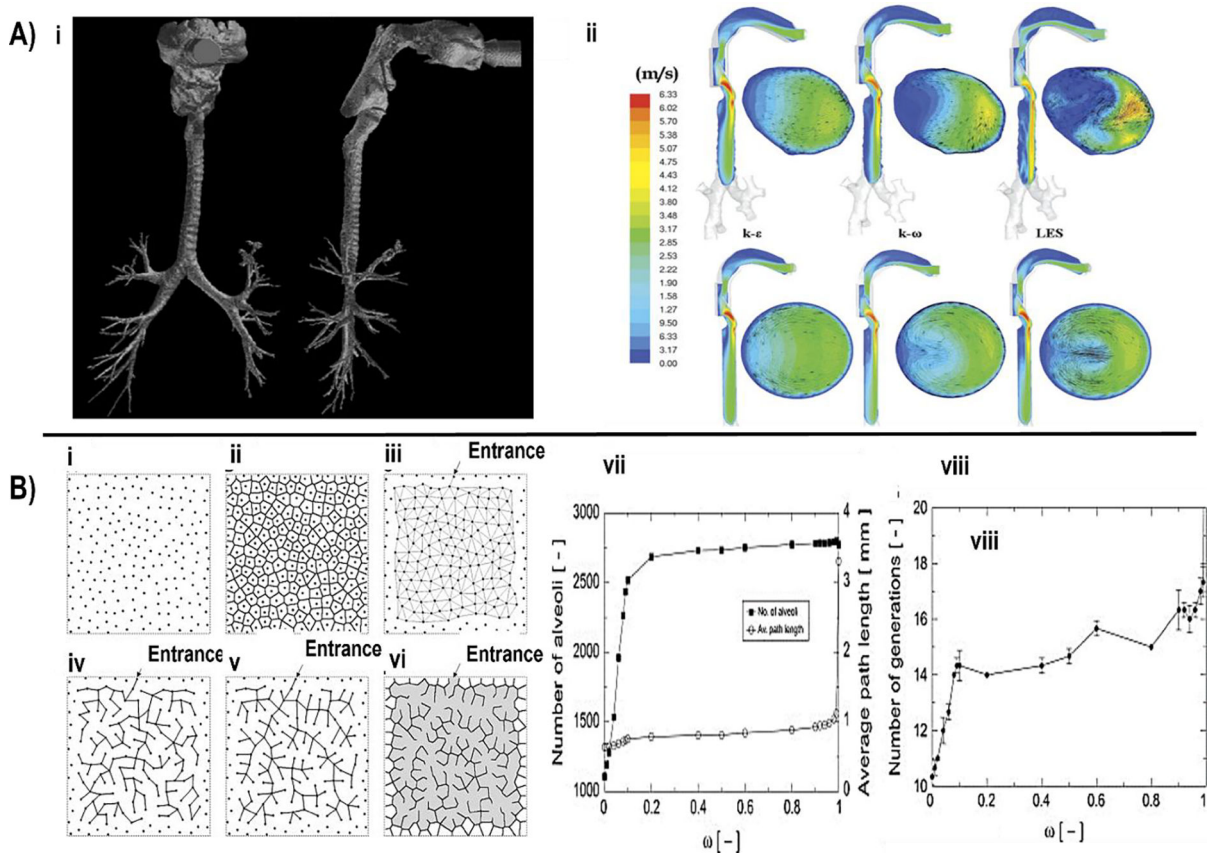


Figure 5.

In silico modelling examples: A) Schematic modeling of heterogeneous acinus structures, i) random seed distribution, ii) Voronoi diagram, iii) Delaunay diagram, iv) initial ductal tree structure, v) optimized ductal tree structure, vi) the resultant acinus structure model, vii) effect of cost weight on the quantity of alveoli and the average route length, the maximum number of generations and viii) for minimum distance between seeds (D_{min}) = 40 (adapted and reproduced with permission from¹⁷⁶). B) i) An image of the oropharynx and airways taken from a CT scan for the sixth generation of bifurcation. For CFD calculations, the image was meshed and transformed to a volume. ii) Velocity contours in three turbulence models (from left to right: k-ε, k-ω and Large Eddy Simulation (LES)) and two geometric models of the airway tree (upper panels: CT based, lower panels: Weibel dimension based) (adapted and reproduced with permission from¹⁷²).

Table 1.

List of ongoing clinical trials obtained using the keyword “Lung Diseases” and “Bioengineering” from [ClinicalTrials.gov](https://clinicaltrials.gov) (Source: <https://clinicaltrials.gov/>, accessed 07.14.22)

	NCT Number / Status	Title	Conditions	Interventions	Characteristics	Sponsor/ Collaborators	Indexed publications
1	NCT03641677 Recruiting	Increasing Lung Transplant Availability Using Normothermic Ex Vivo Lung Perfusion (EVLV) at a Dedicated EVLP Facility	<ul style="list-style-type: none"> • Lung Diseases 	<ul style="list-style-type: none"> • Device: Centralized Lung Evaluation System • Procedure: Lung Transplant 	Study Type: Interventional Phase: Not Applicable	<ul style="list-style-type: none"> • Lung Bioengineering Inc. 	No results posted
2	NCT02234128 Completed	Extending Preservation and Assessment Time of Donor Lungs Using the Toronto EVLP System™ at a Dedicated EVLP Facility	<ul style="list-style-type: none"> • Lung Disease 	<ul style="list-style-type: none"> • Device: Toronto EVLP System™ 	Study Type: Interventional Phase: Not Applicable	<ul style="list-style-type: none"> • Lung Bioengineering Inc. 	[197]
3	NCT04825067 Recruiting	Remote Monitoring of High-Risk Patients with Chronic Cardiopulmonary Diseases	<ul style="list-style-type: none"> • Congestive Heart Failure • Asthma • Chronic Obstructive Pulmonary Disease • Cystic Fibrosis 	<ul style="list-style-type: none"> • Device: Respiratory Sensor measurements 	Study Type: Interventional Phase: Not Applicable	<ul style="list-style-type: none"> • Institute of Bioengineering and Bioimaging (IBB) • Massachusetts General Hospital 	No results posted
4	NCT03993002 Terminated (Enrollment pause due to COVID-19)	DAMP-Mediated Innate Immune Failure and Pneumonia After Trauma - the Harvard-Longwood (HALO) Campus Area Consortium	<ul style="list-style-type: none"> • Respiratory Failure 	<ul style="list-style-type: none"> • Other: Normoxia with Normocarbica • Other: Normoxia with Hypercarbica • Other: Hyperoxia with Normocarbica • Other: Hyperoxia with Hypercarbica 	Study Type: Interventional Phase: Not Applicable	<ul style="list-style-type: none"> • Beth Israel Deaconess Medical Center • United States Department of Defense 	No results posted
5	NCT00805246 Completed	Assessing the Prognosis of Pulmonary Embolism Using Clinical and Imaging Biomarkers (Retrospective & Prospective)	<ul style="list-style-type: none"> • Pulmonary Embolism 		Study Type: Observational Phase:	<ul style="list-style-type: none"> • University of Pittsburgh • National Institutes of Health (NIH) • National Heart, Lung, and Blood Institute (NHLBI) 	No results posted
6	NCT03217240 Unknown status	Integrated Computational Modeling of Right Heart Mechanics and Blood Flow Dynamics in Congenital Heart Disease	<ul style="list-style-type: none"> • Congenital Heart Disease • Pulmonary Hypertension 	<ul style="list-style-type: none"> • Procedure: Cardiac Magnetic Resonance - MRI • Other: Cardiopulmonary Exercise Test • Other: Blood Sampling for all participants 	Study Type: Observational Phase:	<ul style="list-style-type: none"> • National Heart Centre Singapore • Ministry of Health, Singapore 	[198199]
7	NCT04254497 Completed	A Comprehensive Evaluation of Circulating Tumor DNA and	<ul style="list-style-type: none"> • Lung Cancer 	<ul style="list-style-type: none"> • Diagnostic Test: EGFR mutation detection kit 	Study Type: Observational Phase:	<ul style="list-style-type: none"> • Changi General Hospital 	No results posted

	NCT Number / Status	Title	Conditions	Interventions	Characteristics	Sponsor/ Collaborators	Indexed publications
		Circulating Tumor Cells as a Predictive Marker in Lung Cancer					
8	NCT03564522 Active, not recruiting	Image-based Multi-scale Modeling Framework of the Cardiopulmonary System: Longitudinal Calibration and Assessment of Therapies in Pediatric Pulmonary Hypertension	<ul style="list-style-type: none"> • Pulmonary Hypertension • Congenital Heart Disease • Pediatric Congenital Heart Disease 	<ul style="list-style-type: none"> • Procedure: Cardiac catheterization • Radiation: Cardiac MRI 	Study Type: Observational Phase:	<ul style="list-style-type: none"> • University of Michigan • Michigan State University • Nationwide Children's Hospital • National Heart, Lung, and Blood Institute (NHLBI) 	No results posted
9	NCT01795742 Completed	Equivalence of a Human-Powered Nebulizer to an Electric Nebulizer	<ul style="list-style-type: none"> • Asthma 	<ul style="list-style-type: none"> • Device: Human-Powered Nebulizer 	Study Type: Interventional Phase: Phase 2	<ul style="list-style-type: none"> • Marquette University 	[²⁰⁰]
10	NCT03149341 Enrolling by invitation	MRI and Computational Simulation Cardiology Study	<ul style="list-style-type: none"> • Congenital Heart Disease • Pulmonary Hypertension 	<ul style="list-style-type: none"> • Other: Magnetic Resonance Imaging 	Study Type: Observational Phase:	<ul style="list-style-type: none"> • Stanford University 	No results posted
11	NCT02141191 Completed	A Study of Lung Clearance After Hypertonic Saline Delivery Using the tPAD Device	<ul style="list-style-type: none"> • Cystic Fibrosis 	<ul style="list-style-type: none"> • Drug: Inhaled hypertonic saline (7%) 	Study Type: Interventional Phase: Phase 1	<ul style="list-style-type: none"> • University of Pittsburgh • Parion Sciences 	No results posted
12	NCT00248755 Completed	Assessing Mucociliary Clearance and Airway Liquid Volume in the CF Airway	<ul style="list-style-type: none"> • Cystic Fibrosis 	<ul style="list-style-type: none"> • Procedure: Mucociliary clearance scan 	Study Type: Interventional Phase: Not Applicable	<ul style="list-style-type: none"> • University of Pittsburgh • Cystic Fibrosis Foundation 	[²⁰¹]
13	NCT03007875 Completed	High-activity Natural Killer Immunotherapy for Small Metastases of Non-small Cell Lung Cancer	<ul style="list-style-type: none"> • Non-small Cell Lung Cancer • Metastatic 	<ul style="list-style-type: none"> • Biological: High-activity natural killer 	Study Type: Interventional Phase: <ul style="list-style-type: none"> • Phase 1 • Phase 2 	<ul style="list-style-type: none"> • Fuda Cancer Hospital, Guangzhou • Shenzhen Hank Bioengineering Institute 	No results posted
14	NCT02843815 Completed	Combination of Cryosurgery and NK Immunotherapy for Advanced Non-Small Cell Lung Cancer	<ul style="list-style-type: none"> • Non-small Cell Lung Cancer • Metastatic 	<ul style="list-style-type: none"> • Device: Cryosurgery • Biological: NK Immunotherapy 	Study Type: Interventional Phase: <ul style="list-style-type: none"> • Phase 1 • Phase 2 	<ul style="list-style-type: none"> • Fuda Cancer Hospital, Guangzhou • Shenzhen Hank Bioengineering Institute 	[²⁰²]
15	NCT02845856 Completed	Combination of Cetuximab and NK Immunotherapy for Recurrent Non-small Cell Lung Cancer	<ul style="list-style-type: none"> • Recurrent Non-small Cell Lung Cancer 	<ul style="list-style-type: none"> • Drug: Cetuximab • Biological: NK immunotherapy 	Study Type: Interventional Phase: <ul style="list-style-type: none"> • Phase 1 • Phase 2 	<ul style="list-style-type: none"> • Fuda Cancer Hospital, Guangzhou • Shenzhen Hank Bioengineering Institute 	No results posted
16	NCT03847519 Recruiting	Study of ADXS-503 With or Without Pembrolizumab in Subjects with Metastatic Non-	<ul style="list-style-type: none"> • Lung Cancer, Non-Small Cell • Metastatic Squamous Cell Carcinoma • Metastatic 	<ul style="list-style-type: none"> • Drug: ADXS-503 • Drug: Pembrolizumab 	Study Type: Interventional Phase: <ul style="list-style-type: none"> • Phase 1 • Phase 2 	<ul style="list-style-type: none"> • Advaxis, Inc. 	[²⁰³]

	NCT Number / Status	Title	Conditions	Interventions	Characteristics	Sponsor/ Collaborators	Indexed publications
		Small Cell Lung Cancer	Non-Squamous Cell Carcinoma				
17	NCT02232841 Completed	Electrical Impedance Imaging of Patients on Mechanical Ventilation	<ul style="list-style-type: none"> • Pneumothorax • Pulmonary Contusion • Pleural Effusion • Pulmonary Edema • Atelectasis • Hyperinflation • Emphysema • Acute Respiratory Distress Syndrome 	<ul style="list-style-type: none"> • Device: Mechanical Ventilation • Device: CT Scan 	Study Type: Observational Phase:	<ul style="list-style-type: none"> • Colorado State University • National Institute for Biomedical Imaging and Bioengineering (NIBIB) 	[²⁰⁴]
18	NCT05452005 Recruiting	Fluorine-18-AlphaVBeta6-Binding Peptide Positron Emission Tomography in Metastatic Non-Small Cell Lung Cancer	<ul style="list-style-type: none"> • Lung Cancer • Lung Cancer Metastatic • Brain Metastases • Non Small Cell Lung Cancer 	• Drug: 18F- ¹⁸ F-#v#6-BP	Study Type: Interventional Phase: Phase 1	<ul style="list-style-type: none"> • University of California, Davis • United States Department of Defense 	No results posted
19	NCT01987271 Completed	Effects Of Noninvasive Ventilation on Functional Capacity of Patients with Cystic Fibrosis	• Cystic Fibrosis	• Device: Noninvasive Ventilation	Study Type: Interventional Phase: Not Applicable	<ul style="list-style-type: none"> • Universidade Federal de Pernambuco • Coordenação de Aperfeiçoamento de Pessoal de Nível Superior. 	[²⁰⁵]
20	NCT04973371 Completed	Acceptability and Feasibility of Home-based TB Testing	<ul style="list-style-type: none"> • Tuberculosis, Pulmonary • Households 	• Diagnostic Test: Home-based point-of-care (POC) TB testing using GeneXpert device + MTB/RIF test	Study Type: Interventional Phase: Not Applicable	<ul style="list-style-type: none"> • Foundation for Professional Development (Pty) Ltd • National Institutes of Health (NIH) • National Institute for Biomedical Imaging and Bioengineering (NIBIB) • Medical Research Council, South Africa • Foundation for Innovative New Diagnostics, Switzerland • University of Witwatersrand, South Africa • University of California, Irvine 	No results posted
21	NCT04878445 Recruiting	Tissue Engineering Approaches to Treat COPD	Lung Cancer	Procedure: Patients undergoing standard surgery, excess tissue only will be analyzed	Study Type: Interventional Phase: Not Applicable	University Hospitals of North Midlands NHS Trust	No results posted

	NCT Number / Status	Title	Conditions	Interventions	Characteristics	Sponsor/ Collaborators	Indexed publications
				with patient consent.			

Author Manuscript

Author Manuscript

Author Manuscript

Author Manuscript